AD NUMBER

AD824952

LIMITATION CHANGES

TO:

Approved for public release; distribution is unlimited.

FROM:

Distribution authorized to U.S. Gov't. agencies and their contractors; Critical Technology; JAN 1968. Other requests shall be referred to NASA , Goddard Space Flight Center, Greenbelt, MD. This document contains export-controlled technical data.

AUTHORITY

AEDC ltr, 4 Apr 1973

AEDC-TR-67-256

cy 1

QUALIFICATION TESTS OF THIOKOL CHEMICAL CORPORATION TE-M-364-3 SOLID-PROPELLANT ROCKET MOTORS TESTED IN THE SPIN AND NO-SPIN MODE AT SIMULATED ALTITUDE CONDITIONS (PART II - FINAL PHASE)

D. W. White and J.E. Harris

ARO, Inc.

January 1968

This document is subject to special export controls and each transmittal to foreign governments or foreign nationals may be made only with prior approval of NASA, Goddard Space Flight Center, Greenbelt, Maryland.

ROCKET TEST FACILITY

ARNOLD ENGINEERING DEVELOPMENT CENTER

AIR FORCE SYSTEMS COMMAND

ARNOLD AIR FORCE STATION, TENNESSEE

NOTICES

When U. S. Government drawings specifications, or other data are used for any purpose other than a definitely related Government procurement operation, the Government thereby incurs no responsibility nor any obligation whatsoever, and the fact that the Government may have formulated, furnished, or in any way supplied the said drawings, specifications, or other data, is not to be regarded by implication or otherwise, or in any manner licensing the holder or any other person or corporation, or conveying any rights or permission to manufacture, use, or sell any patented invention that may in any way be related thereto.

Qualified users may obtain copies of this report from the Defense Documentation Center.

References to named commercial products in this report are not to be considered in any sense as an endorsement of the product by the United States Air Force or the Government.

QUALIFICATION TESTS OF THIOKOL CHEMICAL CORPORATION TE-M-364-3 SOLID-PROPELLANT ROCKET MOTORS TESTED IN THE SPIN AND NO-SPIN MODE AT SIMULATED ALTITUDE CONDITIONS (PART II - FINAL PHASE)

D. W. White and J. E. Harris
ARO, Inc.

AF—AEDC
Arnold AFB Tenn

FOREWORD

The test program reported herein was conducted under the sponsorship of the National Aeronautics and Space Administration (NASA), Goddard Space Flight Center (GSFC), for the Thiokol Chemical Corporation (TCC), Elkton Division, under System 921E, Project 9033.

The results of the test were obtained by ARO, Inc. (a subsidiary of Sverdrup & Parcel and Associates, Inc.), contract operator of the Arnold Engineering Development Center (AEDC), Air Force Systems Command (AFSC), Arnold Air Force Station, Tennessee, under Contract No. AF 40(600)-1200. The test was conducted in Propulsion Engine Test Cell (T-3) of the Rocket Test Facility (RTF) from August 9 to 30, 1967, under ARO Project Number RC1707, and the manuscript was submitted for publication on November 2, 1967.

Information in this report is embargoed under the Department of State International Traffic in Arms Regulations. This report may be released to foreign governments by departments or agencies of the U. S. Government subject to approval of NASA, Goddard Space Flight Center, or higher authority. Private individuals or firms require a Department of State export license.

This technical report has been reviewed and is approved.

Edward C. Westwood	Leonard T. Glaser
Captain, USAF	Colonel, USAF
Acting AF Representative, RTF	Director of Test
Directorate of Test	

ABSTRACT

A qualification test program consisting of six Thiokol Chemical Corporation TE-M-364-3 solid-propellant rocket motors was conducted at near vacuum conditions to determine altitude ballistic performance, nonaxial thrust of the spinning motors, tailoff characteristics, temperature-time history during and after motor operation, and component structural integrity. The initial phase of the program consisted of firing one motor in the spin mode and one motor in the no-spin mode. The final phase consisted of firing three motors in the spin mode and one motor in the no-spin mode. The vacuum total impulse values of all motors were within the specification limits. Nonaxial thrust impulse values of the spinning motors and the maximum motor case temperatures for all motors exceeded the specification limit.

CONTENTS

APPENDIXES

I. ILLUSTRATIONS

Figure

NOMENCLATURE

$A_{ex_{avg}}$	Average of pre- and post-fire nozzle exit area, $in.^2$
$At_{post\text{-}fire}$	Post-fire nozzle throat area, $in.^2$
C_F	Vacuum thrust coefficient
c_f	Thrust coefficient over a selected 1-sec interval
F	Measured thrust, lb_f
P_{cell}	Measured cell pressure, psia
P_{ch}	Measured chamber pressure, psia
P_{max}	Maximum chamber pressure developed during normal motor operation, excluding ignition spike, psia
t_a	Action time, time interval between 10 percent of maximum chamber pressure during ignition and 10 percent of maximum chamber pressure during tailoff, sec
t_{bd}	Time of nozzle flow breakdown (indicated by increase in cell pressure), sec
t_i	Time of first increase in chamber pressure at motor ignition, sec
t_{it}	Total burn time, interval from time of increase in chamber pressure during ignition until chamber pressure has decreased to cell pressure during tailoff, sec
t_{is}burn time	Time interval from time of increase in chamber pressure during ignition until the ratio of chamber pressure to test cell pressure has decreased to 1.3 during tailoff, sec
t_ℓ	Ignition lag time, interval from zero time to time of increase in chamber pressure, sec
t_o	Zero time, time at which firing voltage is applied to the igniter circuit, sec
t_s	Nozzle throat flow goes subsonic, time at which the ratio of chamber pressure to test cell pressure has decreased to 1.3 during tailoff, sec
t_t	Time at which chamber pressure equals cell pressure during tailoff, sec

SECTION I
INTRODUCTION

The Thiokol Chemical Corporation (TCC) TE-M-364-3 solid-propellant rocket motor is to be used as the third stage of the Improved Delta Launch Vehicle, DSV-3M (Fig. 1, Appendix I). Delta missions scheduled to utilize the TE-M-364-3 motor include Radio Astronomy Explorer (RAE), Interim Defense Communications Satellite program (IDSEP) International Tele-communications Satellite Program (Intelsat III), and the Tiros Operational Satellite (Tiros M) (Ref. 1). For each of these third-stage and payload combinations, attitude control will be achieved by spin stabilization.

A qualification test program consisting of six TCC TE-M-364-3 motors was to be conducted at near vacuum conditions. The initial phase of the program consisted of firing one motor in the spin mode and one motor in the no-spin mode. The results of the initial phase of testing are presented in Ref. 2 and discussed in Section IV.

The primary objectives of the final phase reported herein were to fire one motor in the no-spin mode and three motors while spinning about their centerlines at 110 rpm to determine altitude ballistic performance, nonaxial thrust of the spinning motors, tailoff characteristics, temperature-time history during and after motor operation, and component structural integrity. The motors were temperature conditioned at prescribed temperature levels of 50, 55, 75, and 95 ± 5°F for a minimum of 46 hr prior to firing.

Motor altitude ballistic performance, nonaxial thrust measurements, tailoff characteristics, temperature-time history, and structural integrity are discussed.

SECTION II
APPARATUS

2.1 TEST ARTICLE

The TCC TE-M-364-3 solid-propellant rocket motor (Fig. 2) is a full-scale flightweight motor having the following nominal dimensions and burning characteristics at 75°F:

Length, in.	53
Diameter, in.	37
Loaded Weight, lb_m	1580
Propellant Weight, lb_m	1440
Throat Area, $in.^2$	8.50
Nozzle Area Ratio, A/A*	53:1
Maximum Thrust, lb_f	10,970
Maximum Chamber Pressure, psia	650
Burn Time, sec	40

The cylindrical motor case is constructed of 0.040-in. steel. The aft hemisphere and approximately one-half of the forward hemisphere regions are insulated with V-44 asbestos-filled Buna-N® rubber. The remaining case area is uninsulated (Fig. 2a). Two 37-in.-diam thrust attachment flanges are located near the motor equator.

The contoured nozzle assembly contains a Graph-I-Tite G-90 carbon throat insert and an expansion cone constructed of outer layers of glass cloth phenolic and inner layers of carbon cloth phenolic. The partially submerged nozzle assembly has a nominal 53:1 area ratio (A/A*) and a 15-deg half-angle at the exit plane. Eight aluminum antenna studs and a fiber glass stiffner (support) ring are normally bonded to the nozzle expansion cone adjacent to the exit plane. For motors S/N T00003 and S/N T00006, the existing nozzles were modified by removing the antenna studs and the fiber glass bands, shortening the expansion cones at the exit plane by 0.161 in., and thereby increasing the exit cone thickness at the exit plane from 0.094 to 0.134 in. The fiber glass bands were replaced with carbon roving bands which were pre-impregnated with a modified phenolic resin (Fig. 2a).

The TE-M-364-3 rocket motor contains a propellant grain formulation designated TP-H-3062 (ICC Class B), which is cast in an eight-point-star configuration (Fig. 2b). The isentropic exponent of the propellant exhaust gases is 1.18 (assuming frozen equilibrium).

Ignition was accomplished by a TE-P-358-3 Pyrogen® igniter (Fig. 3), which contained 19 gm of size 2A boron pellets used to initiate the eight-point-star igniter grain. The aft section of the igniter culminated in a nozzle body containing six small nozzles for distribution of the igniter propellant flame onto the motor propellant grain (Fig. 2a). The head end of the igniter contained a mechanical safe and arm device, two squib ports, one pyrogen pressure port, and one chamber pressure port. One McCormick Selph® nominal 15-sec delay squib was used for the tests reported herein except for motor S/N T00002 for which two squibs were used. Nominal ignition current was 5 amp/squib and was maintained for approximately 0.3 sec.

2.2 INSTALLATION

The motors were cantilever mounted from the spindle face of a spin fixture assembly in Propulsion Engine Test Cell (T-3) (Ref. 3). The spin assembly was mounted on a thrust cradle, which was supported from the cradle support stand by three vertical and two horizontal double-flexure columns (Fig. 4). The spin fixture assembly consists of a 10-hp squirrel-cage-type drive motor, a forward thrust bearing assembly, a 46-in.-long spindle having a 36-in.-diam aft spindle face, and an aft bearing assembly. Each motor was secured in a mounting can which was adapted to the spindle face. For the spin firings, the spin fixture was rotated counterclockwise, looking upstream. For the no-spin firing the spin fixture was locked in place to prevent rotation. Electrical leads to and from the igniters, pressure transducers, and thermocouples on both motors were provided through a 170-channel, slip-ring assembly mounted between the forward and aft bearing assemblies on the spindle. Axial thrust was transmitted through the spindle-thrust bearing assembly to two load cells mounted just forward of the thrust bearing.

Pre-ignition pressure altitude conditions were maintained in the test cell by a steam ejector operating in series with the RTF exhaust gas compressors. During a motor firing, the motor exhaust gases were used as the driving gas for the 42-in.-diam, ejector-diffuser system to maintain test cell pressure at an acceptable level.

2.3 INSTRUMENTATION

Instrumentation was provided to measure axial thrust, nonaxial force, Pyrogen pressure, motor chamber pressure, test cell pressure, motor case and nozzle temperatures, and rotational speed. Table I (Appendix II) presents range of measurements, recording methods, and an estimate of measurement uncertainty for all reported parameters.

The axial thrust measuring system consisted of two double-bridge, strain-gage-type load cells mounted in the axial double-flexure column forward of the thrust bearing on the spacecraft centerline. The nonaxial force measuring system consisted of double-bridge, strain-gage-type load cells installed forward and aft between the flexure-mounted cradle and the cradle support stand.

The load cells were installed on the rocket motor axial centerline and in the horizontal plane passing through the motor centerline (Fig. 4c).

Unbonded strain-gage-type transducers were used to measure test cell pressure. Bonded strain-gage-type transducers with ranges of 0 to 5, 0 to 15, 0 to 50, 0 to 750, and 0 to 1500 psia were used to measure motor chamber pressure and Pyrogen pressure. Chromel®-Alumel® (CA) thermocouples were bonded to the motor case and nozzle (Fig. 5) to measure outer surface temperatures during and after motor burn time. Rotational speed of the motor assembly was determined from the output of a magnetic pickup.

The output signal of each measuring device was recorded on independent instrumentation channels. Ballistic data were obtained from four axial thrust channels, three test cell pressure channels, two Pyrogen pressure channels, and five motor chamber pressure channels. These data were recorded as follows: Each instrument output signal was indicated in totalized digital form on a visual readout of a millivolt-to-frequency converter. A magnetic tape system, recording in frequency form, stored the signal from the converter for reduction at a later time by an electronic digital computer. The computer provided a tabulation of average absolute values for each 0.10-sec time increment and total integrals over the cumulative time increments.

The output signal from the magnetic rotational speed pickup was recorded in the following manner: A frequency-to-analog converter was triggered by the pulse output from the magnetic pickup and in turn supplied a square wave of constant amplitude to the electronic counter and oscillograph recorder. The scan sequence of the electronic counter was adjusted so that it displayed directly the motor spin rate in revolutions per minute.

The millivolt outputs of the thermocouples were recorded on magnetic tape from a multi-input, analog-to-digital converter at a sampling rate for each thermocouple of 150 samples per second. The millivolt outputs of the nonaxial force load cells were recorded on FM analog magnetic tape and played back through a filter system to an oscillograph and a digital magnetic tape recorder at a later time.

A recording oscillograph was used to provide an independent back-up of all operating instrumentation channels except the temperature and nonaxial force systems. Selected channels of thrust and pressures were recorded on null-balance potentiometer-type strip charts for analysis immediately after a motor firing. Visual observation of each firing was provided by a closed-circuit television monitor. High-speed, motion-picture cameras provided a permanent visual record of each firing.

The thrust calibrator weights, axial and nonaxial force load cells, and pressure transducers were laboratory calibrated prior to usage in this program. After installation of the measuring devices in the test cell, all systems were calibrated at ambient conditions and again at simulated altitude conditions just before a motor firing.

The pressure systems were calibrated by an electrical, four-step calibration, using resistances in the transducer circuits to simulate selected pressure levels. The axial thrust instrumentation systems were calibrated by applying to the thrust cradle known forces which were produced by deadweights acting through a bell crank. The calibrator is hydraulically actuated and remotely operated from the control room. The nonaxial force instrumentation systems were calibrated by an electrical, four-step calibration, using resistances in the circuits to simulate selected force levels. Thermocouple systems were calibrated by using known millivolt levels to simulate selected thermocouple outputs.

After each motor firing, with the test cell still at simulated altitude pressure, the systems were again recalibrated to determine if any shift had occurred.

SECTION III
PROCEDURE

The four TCC TE-M-364-3 rocket motors (S/N's T00001, T00002, T00003, and T00006) arrived at AEDC between April 10 and August 10, 1967. The motors were visually inspected for possible shipping damage and radiographically inspected at about 75°F for grain cracks, voids, or separation and found to meet criteria provided by the manufacturer. (Prior to installing motor S/N T00006 in the test cell, the motor was subjected to a temperature environment of 40°F for 46 hr and then X-rayed again at the cold temperature to determine temperature effects on the propellant-to-insulator bonding. The X-rays did not reveal any propellant-to-insulator separations.) During storage in an area temperature conditioned at 75 ± 5°F, the motors were checked to ensure correct fit of mating hardware, and the electrical resistances of the igniters were measured. The nozzle throat and exit diameters were obtained, and the motors were weighed. Thermocouples were bonded to the nozzle and motor case, the pressure manifold with transducers were mounted, and the entire motor assembly was photographed and installed in the firing can.

Dimensions of selected surfaces as a function of angular position relative to the centerline of the spin motors (S/N's T00001, T00002, and T00006) were determined by TCC personnel to facilitate alignment of the motors in the test cell.

3.1 NO-SPIN MOTOR

After installation of the no-spin motor (S/N T00003) in the test cell, instrumentation connections were made, and the spin fixture was locked in place to prevent rotation. The motor was temperature conditioned for a period in excess of 46 hr prior to closing the test cell; during this time a continuity check of all electrical systems was performed. Pre-fire ambient calibrations were completed, the test cell pressure was reduced to simulate the desired altitude, and altitude calibrations were taken.

The final operation prior to firing the motor was to adjust the firing circuit resistance to provide the desired current (5 amp) to the igniter squib. The entire instrumentation measuring-recording complex was activated, and the motor was fired. Simulated altitude conditions were maintained for approximately 45 min after the firing, during which time motor temperatures were recorded and post-fire calibrations were completed. Low-range chamber pressure data were also recorded for 10 min after burnout of the motor. The test cell pressure was then returned to ambient conditions, and the motor was inspected, photographed, and removed to the storage area. Post-fire inspections at the storage area consisted of measuring the throat and exit diameters of the nozzle, weighing the motor, and photographically recording the post-fire condition of the motor.

3.2 SPIN MOTORS

The procedure for the spin motors was identical to that for the no-spin motor, with the following exceptions:

a. The motor centerlines were axially aligned with the spin axis by rotating the motors and measuring the deflection of the selected motor surfaces with a dial indicator and making appropriate adjustments.

b. The assembly was balanced at a rotational speed of 110 rpm, and in-place stand static and dynamic calibrations were accomplished (see Appendix III).

c. Pre-fire altitude calibrations were made after spinning of the motor assembly had stabilized at 110 rpm.

d. The motors were fired while spinning (under power) at 110 rpm.

e. Spinning of the motor was continued for approximately 40 min after burnout, during which time the post-fire altitude calibrations were made.

SECTION IV
RESULTS AND DISCUSSION

Four Thiokol Chemical Corporation (TCC) TE-M-364-3 solid-propellant rocket motors (S/N's T00001, T00002, T00003, and T00006) were fired in Propulsion Engine Test Cell (T-3). The motors were pre-fire temperature conditioned at 55 ± 5°F (S/N T00001), 95 ± 5°F (S/N T00002), 75 ± 5°F (S/N T00003), and 50 ± 5°F (S/N T00006) for periods in excess of 46 hr and fired at average pressure altitudes of about 104,000 ft (88,000 ft for S/N T00002). Motor S/N T00003 was fired in the no-spin mode. The remaining three motors were fired while spinning about their motor centerlines at about 110 rpm. The primary objectives of the tests reported herein were to fire one motor in the no-spin mode and three motors while spinning about their centerlines at 110 rpm to determine altitude ballistic performance, nonaxial thrust of the spinning motors, tailoff characteristics, temperature-time history during and after motor operation, and component structural integrity. Prior to receipt of motors S/N's T00001 and T00002 at AEDC, they were subjected to the following environmental treatment.

a. Both motors were temperature cycled between 40 and 100 ± 5°F for three complete cycles. Half-cycle duration was 46 hr minimum.

b. Both motors were drop tested while packaged in their shipping containers in a temperature environment of 70 ± 30°F. The drop test consisted of placing one side of the shipping container on 6-in.-high chocks and elevating the other side of the container 24 in. and releasing. The test was repeated after reversing sides of the container.

c. Both motors were subjected to sinusoidal sweep vibration testing in each of three mutually perpendicular axes as follows:

Axis	Frequency, Hz	Level
Lateral and Transverse	5 to 8	0.5-in. double amplitude
	8 to 200	3.5 g peak-to-peak
Axial	8 to 13	0.5-in. double amplitude
	13 to 16	9.0 g peak-to-peak
	16 to 32	7.0 g peak-to-peak
	32 to 200	3.0 g peak-to-peak

For the vibrational testing, motor S/N T00001 was temperature conditioned at 40 ± 5°F, whereas motor S/N T00002 was temperature conditioned at 100 ± 5°F.

Data from the four motor tests are presented in both tabular and graphical form. A summary of motor physical dimensions is presented in Table II. Motor performance data, based on action time (t_a) and t_{is} burn time, are summarized in Table III. Specific impulse values are presented using both the manufacturer's stated propellant weight and the motor expended mass determined from pre- and post-fire motor weights. When multiple channels of equal accuracy instrumentation data were used to obtain values of a single parameter, the average value was used to calculate the data presented.

4.1 ALTITUDE IGNITION CHARACTERISTICS

The motors were ignited at pressure altitudes ranging from 112,000 to 124,000 ft. An analog trace of a typical ignition event is shown in Fig. 6. Ignition lag time increased from 14.815 to 15.948 sec as prefire grain temperature decreased from 95 to 50°F. The igniter utilized a nominal 15-sec delay squib (two squibs for motor S/N T00002). Peak Pyrogen pressures during the ignition events varied from 1179 to 1254 psia.

4.2 ALTITUDE BALLISTIC PERFORMANCE

The variations of thrust, chamber pressure, and test cell pressure for each motor fired are shown in Fig. 7. The variations of chamber pressure, measured with a 0- to 15- or a 0- to 5-psia transducer,

and test cell pressure during an extended portion of tailoff for each motor fired are presented in Fig. 8.

Since the nozzle does not operate fully expanded at the low chamber pressures encountered during tailoff burning, the measured total impulse data during this period cannot be corrected to vacuum conditions by adding the product of cell pressure integral and nozzle exit area. Therefore, total burn time (t_{it}) was segmented (Fig. 9), and the method used to determine vacuum impulse is described as follows: The time of exhaust nozzle flow breakdown (t_{bd}) was considered to have occurred simultaneously with the time of exhaust diffuser flow breakdown (as indicated by the sudden increase in cell pressure). After this time, flow at the nozzle throat was considered to be at sonic velocity until the time (t_s) at which the ratio of motor chamber pressure to cell pressure had decreased to a value of 1.3.

Vacuum corrected total impulse data were then calculated from:

$$I_{vac} = \int_{t_i}^{t_{bd}} F dt + A_{ex|_{avg}} \int_{t_i}^{t_{bd}} P_{cell}\, dt + \bar{c}_f A_{t(post)} \int_{t_{bd}}^{t_s} P_{ch}\, dt$$

where

$$\bar{c}_f = \frac{\int_{t_1}^{t_2} F\, dt - A_{ex(post)} \int_{t_1}^{t_2} P_{cell}\, dt}{A_{t(post)} \int_{t_1}^{t_2} P_{ch}\, dt}$$

$$= 1.848 \text{ (S/N T00001), } 1.858 \text{ (S/N T00002), } 1.862 \text{ (S/N T00003), and } 1.859 \text{ (S/N T00006).}$$

The time interval (t_1 to t_2) is a one-second interval of motor operation just prior to decrease in chamber pressure (Fig. 9). The impulse accumulated between the time that the nozzle throat flow becomes subsonic (t_s) and the end of burn time (t_t) is considered negligible. Performance characteristics for the four motors are tabulated below along with the performance characteristics of the two previous motor firings reported in Ref. 2:

Parameter	Reported Herein				Ref. 2	
Motor S/N	T00001	T00002	T00003	T00005	T00004	T00006
Pre-Fire Grain Temp, °F	55 ± 5	95 ± 5	75 ± 5	50 ± 5	75 ± 5	75 ± 5
Motor Spin Rate, rpm	110	110	0	110	0	110
Action Time (t_a), sec	45.6	43.5	45.0	46.1	45.2	44.6
t_{is} Burn Time, sec	121.6	100.6	100.6	111.85	111.3	80.3
Total Burn Time (t_{it}), sec	126	124	124	120	140	130
Vacuum Total Impulse Based on t_{is} burn time, lb_f-sec	418,861	419,426	419,531	418 133	418,601	419,724
Vacuum Specific Impulse Based on t_{is} burn time and the Manufacturer's Stated Propellant Weight, lb_f-sec/lb_m	291 00	291 53	291 22	290 39	290.86	291.14
Vacuum Specific Impulse Based on t_{is} burn time and Expended Mass, lb_f-sec/lb_m	288.40	288.94	288.64	287.90	288.20	288.77
Average Vacuum Thrust Coefficient Based on t_a and the Average Pre- and Post-Fire Throat Area, c_f	1.852	1.859	1 854	1.853	*	1.859

*Average vacuum thrust coefficient not available.

Specification values of vacuum total impulse are 417,790, 418,100, and 418,400 lb_f-sec when the TE-M-364-3 motors are fired at 60, 75, and 90°F, respectively (Ref. 4). The above tabulation clearly shows that the vacuum total impulse values of the motors reported herein and in Ref. 2 exceed the values listed in the referenced specification.

As expected, action time values decreased and specific impulse values increased as a result of pre-fire grain temperature increasing from 50 to 95°F.

The low level chamber pressure measured after propellant burnout (approximately 50 sec after motor ignition) is believed to have resulted from residual burning propellant slivers and/or smoldering insulator material. There were no indications of increases in chamber pressure during the long tailoff period. Therefore, it is concluded that the motors did not experience any sporadic burning of propellant slivers after motor burnout. Post-fire inspection of motors S/N's T00002, T00003, and T00006 revealed eight small propellant slivers symmetrically located near the motor equator. No propellant slivers were evident during the post-fire inspection of motor S/N T00001.

A comparison of the thrust variations for the three spin motor firings reported herein and the spin motor firing reported in Ref. 2 as a function of time is presented in Fig. 10. Propellant burn rate as a function of the pre-fire temperature conditioning level of the propellant grains is most evident in Fig. 10. For example, motor S/N T00002, which was pre-fire temperature conditioned at 95 ± 5°F, achieved a maximum thrust level of 10,550 lb_f, whereas motor S/N T00006, which was pre-fire temperature conditioned at 50 ± 5°F, achieved a maximum

thrust level of 10,010 lb_f. Consequently, motor S/N T00002 experienced a shorter burn time (approximately 2 sec) than motor S/N T00006.

4.3 NONAXIAL THRUST VECTOR MEASUREMENTS

One of the primary objectives of this test was to measure motor thrust misalignment during the three spin firings (motors S/N's T00001, T00002, and T00006). This objective was accomplished by measuring the nonaxial component of motor thrust. The recorded nonaxial thrust data were treated as described in Appendix III. These data from ignition to the point of nozzle flow breakdown for the three spin firings are presented in Figs. 11, 12, and 13.

The nonaxial thrust values recorded for the three spin firings exhibited peaks during the thrust buildup and decay portions of motor operation. These values are questionable because of undefined dynamic characteristics of the system during the ignition and tailoff transients. Because of the uncertainties inherent in the data recorded during these transients, they will not be considered in the following discussion.

Nonaxial thrust data for the three spin firings reported herein and the previous spin firing reported in Ref. 2 are presented in the following table. All tabulated parameters are based on data recorded during the time of near steady-state motor operation. This time interval began 1.0 sec after ignition for all four motors and ended 40 sec after ignition for motors S/N's T00002 and T00005 and 42 sec after ignition for motors S/N's T00001 and T00006.

Parameter	Reported Herein			Ref. 2
Motor S/N	T00001	T00002	T00005	T00005
Pre-Fire Grain Temperature, °F	55 ± 5	95 ± 5	50 ± 5	75 ± 3
Average Motor Spin Rate during Firing, rpm	110.97	110.97	111.24	109.30
Time Interval of Near Steady-State Motor Operation, sec	41.0	39.0	41.0	39.0
Maximum Nonaxial Thrust Magnitude, lb_f	12.9	8.0	5.0	11.2
Time of Maximum Nonaxial Force Occurrence (from Ignition), sec	41.9	35.0	32.3	39.6
Angular Location of Maximum Nonaxial Force (Measured Clockwise, Looking Upstream, from Motor Top-Dead-Center), deg	252	87	96	51
Nonaxial Thrust Integral, lb_f-sec	137	184	143	155
Average Nonaxial Thrust Magnitude, lb_f	4.8	4.7	3.5	4.0
Maximum Misalignment of Motor Thrust Axis from Motor Centerline, deg	0.084	0.060	0.053	0.068

The specification value of nonaxial thrust integral is 125 lb_f-sec (Ref. 4). The above tabulation shows that the nonaxial thrust impulse values of the motor firings reported herein and in Ref. 2 exceed the value listed in the referenced specification.

A comparison of the time variation of nonaxial thrust vector magnitude for the three spin-fired TE-M-364-3 motors reported herein and one spin-fired TE-M-364-3 motor reported in Ref. 2 is presented in Fig. 14. All four motors exhibited similar trends in the magnitude time variation. The magnitude for the three motors reported herein increased rapidly from one value to a higher value approximately 30 sec after ignition. The magnitude for the Ref. 2 motor also increased approximately 30 sec after ignition; however, the increase was gradual from 1.3 lb_f, 32.4 sec after ignition, to 13.0 lb_f, 40.7 sec after ignition.

The nonaxial thrust data presented in Figs. 11 through 13 were corrected for nonaxial force caused by misalignment of the motor on the spin fixture. The angular misalignments of the motor centerline with respect to the spin axis were 0.0066, 0.0202, and 0.0244 deg for motors S/N's T00001, T00002, and T00006, respectively. The respective nonaxial thrust corrections resulting from these angular misalignments were approximately 1.1, 3.5, and 4.2 lb_f at each maximum thrust level.

The inaccuracy of the nonaxial force measuring system (excluding the ignition and tailoff transients) for this test is estimated to be ± 0.80 lb_f (Appendix III).

4.4 STRUCTURAL INTEGRITY

Typical motor case and nozzle temperatures for the four motor firings are presented in Figs. 15 through 18. Maximum motor case temperatures were 903 (S/N T00001), 776 (S/N T00002), 668 (S/N T00003), and 840°F (S/N T00006) occurring approximately 72, 82, 104, and 60 sec after motor ignition, respectively. These maximum temperatures were measured on the uninsulated portion of the forward hemisphere over a propellant grain valley by thermocouples T-2 (S/N T00001), T-18 (S/N T00002), T-17 (S/N T00003), and T-2 (S/N T00006). The motor qualification specification (Ref. 4) states that the external surface of the rocket motor assembly, excluding the nozzle, shall not exceed 500°F at any time from ignition to 150 sec thereafter.

Post-fire examination of the four motors did not reveal any distortion of or thermal damage to the motor cases. However, each motor had several small hot-spots located at or near the motor equator. Motor S/N T00001 also had evidenced eight pronounced hot-spots located just forward of the motor equator on the forward hemisphere (Fig. 19).

Each of the four nozzle exit cones experienced thermal damage as was evidenced by delamination and cracking of the inner layers of carbon cloth phenolic (Fig. 20) and flaking of the outer layers of glass cloth phenolic (Fig. 21). Post-fire examination of the Ref. 2 motors revealed similar thermal damage to the nozzle exit cones. Nozzle throat measurements indicated that erosion had caused an increase of 8.69, 8.88, 11.1, and 8.97 percent from the pre-fire areas of motors S/N's T00001, T00002, T00003, and T00006, respectively.

Prior to firing motors S/N's T00001 and T00002, TCC personnel installed eight metal clamps over the aft surface of the fiber glass bands (located at the exit plane of the nozzle expansion cone). These bands were bolted to the eight antenna studs located on the exterior of the expansion cones (Fig. 2a). Post-fire examination of these motors revealed that the fiber glass bands had become partially detached from the nozzle expansion cones over a portion of the exit planes. However, seven of the eight clamps and antenna studs remained in place for motor S/N T00002, whereas only five of the eight clamps and studs remained in place for motor S/N T00001. These remaining clamps possibly prevented the bands from becoming completely detached from the expansion cones.

Post-fire examination of motors S/N's T00003 and T00006 (which contained the modified nozzle expansion cones, see Section II) revealed that the carbon roving bands had become partially detached from the nozzle expansion cones over a portion of the exit planes.

SECTION V
SUMMARY OF RESULTS

Four Thiokol Chemical Corporation TE-M-364-3 solid-propellant rocket motors were temperature conditioned at 50 (S/N T00006), 55 (S/N T00001), 75 (S/N T00003), and 95 ± 5°F (S/N T00002) for periods in excess of 46 hr and fired at average pressure altitudes of about 104,000 ft (88,000 ft, motor S/N T00002). Motor S/N T00003 was fired in the no-spin mode, whereas motors S/N's T00001, T00002,

and T00006 were fired while spinning about their motor centerlines at 110 rpm. Results are summarized as follows:

1. Vacuum total impulse values during the time that nozzle throat flow was sonic were 418,861 (S/N T00001), 419,426 (S/N T00002), 419,531 (S/N T00003), and 418,133 lb_f-sec (S/N T00006). Specification values ranged from 417,790 for 60°F motor to 418,400 lb_f-sec for a 90°F motor. Corresponding vacuum specific impulse values, based on the manufacturer's stated propellant weight, were 291.00 (S/N T00001), 291.53 (S/N T00002), 291.22 (S/N T00003), and 290.39 lb_f-sec/lb_m (S/N T00006).

2. The maximum nonaxial thrust magnitude during the steady-state portion of motor operation was 12.9 (S/N T00001), 8.0 (S/N T00002), and 9.0 lb_f (S/N T00006) occurring 41.9, 35.0, and 32.3 sec after motor ignition, respectively. Nonaxial thrust impulse values accumulated during the steady-state portion of motor operation were 197, 184, and 143 lb_f-sec. The specification value was 125 lb_f-sec/lb_m.

3. The time intervals from the time at which firing voltage was applied to the igniter circuit to the time of increase in chamber pressure were 15.825 (S/N T00001), 14.815 (S/N T00002), 15.411 (S/N T00003), and 15.948 sec (S/N T00006). (The igniters utilized nominal 15-sec delay squibs.)

4. The time intervals between 10 percent of maximum chamber pressure during ignition and 10 percent of maximum chamber pressure during tailoff (t_a) were 45.6 (S/N T00001), 43.5 (S/N T00002), 45.0 (S/N T00003), and 46.1 sec (S/N T00006).

5. Post-fire examination of the four motors did not reveal any distortion or thermal damage to the motor cases. However, each motor had several hot-spots located near the motor equator, and motor S/N T00001 had eight pronounced hot-spots located on the forward hemisphere. The four nozzle exit cones experienced delamination and cracking of the inner layers of carbon cloth phenolic and flaking of the outer layers of glass cloth phenolic.

6. Post-fire examination of the four motors revealed that the nozzle exit support rings had become partially detached from the expansion cones.

7. Each motor experienced low level pressure operation during tailoff for about 70 (S/N T00001), 50 (S/N T00002), 50 (S/N T00003), and 60 sec (S/N T00006). These low level pressures are believed to have resulted from low pressure level propellant sliver burning and/or smoldering insulation.

8. The maximum motor case temperatures were 903 (S/N T00001), 776 (S/N T00002), 668 (S/N T00003), and 840°F (S/N T00006), occurring about 72, 82, 104, and 60 sec after motor ignition, respectively. The motor specification stated that the motor case should not exceed 500°F at any time from ignition to 150 sec thereafter.

REFERENCES

1. Private Communication with W. R. Schindler, National Aeronautics and Space Administration, Goddard Space Flight Center, Greenbelt, Maryland, June 13, 1967.
2. White, D. W. and Harris, J. E. "Evaluation of Two Thiokol Chemical Corporation TE-M-364-3 Solid-Propellant Rocket Motors Tested in the Spin and No-Spin Mode at Simulated Altitude Conditions." AEDC-TR-67-179, October 1967.
3. Test Facilities Handbook (6th Edition). "Rocket Test Facility, Vol. 2." Arnold Engineering Development Center, November 1966.
4. Douglas Aircraft Specification Number CP00154A.
5. Nelius, M. A. and Harris, J. E. "Measurements of Nonaxial Forces Produced by Solid-Propellant Rocket Motors Using a Spin Technique." AEDC-TR-65-228, November 1965.

APPENDIXES

I. ILLUSTRATIONS
II. TABLES
III. CALIBRATION OF NONAXIAL THRUST VECTOR MEASURING SYSTEM TO DETERMINE SYSTEM ACCURACY

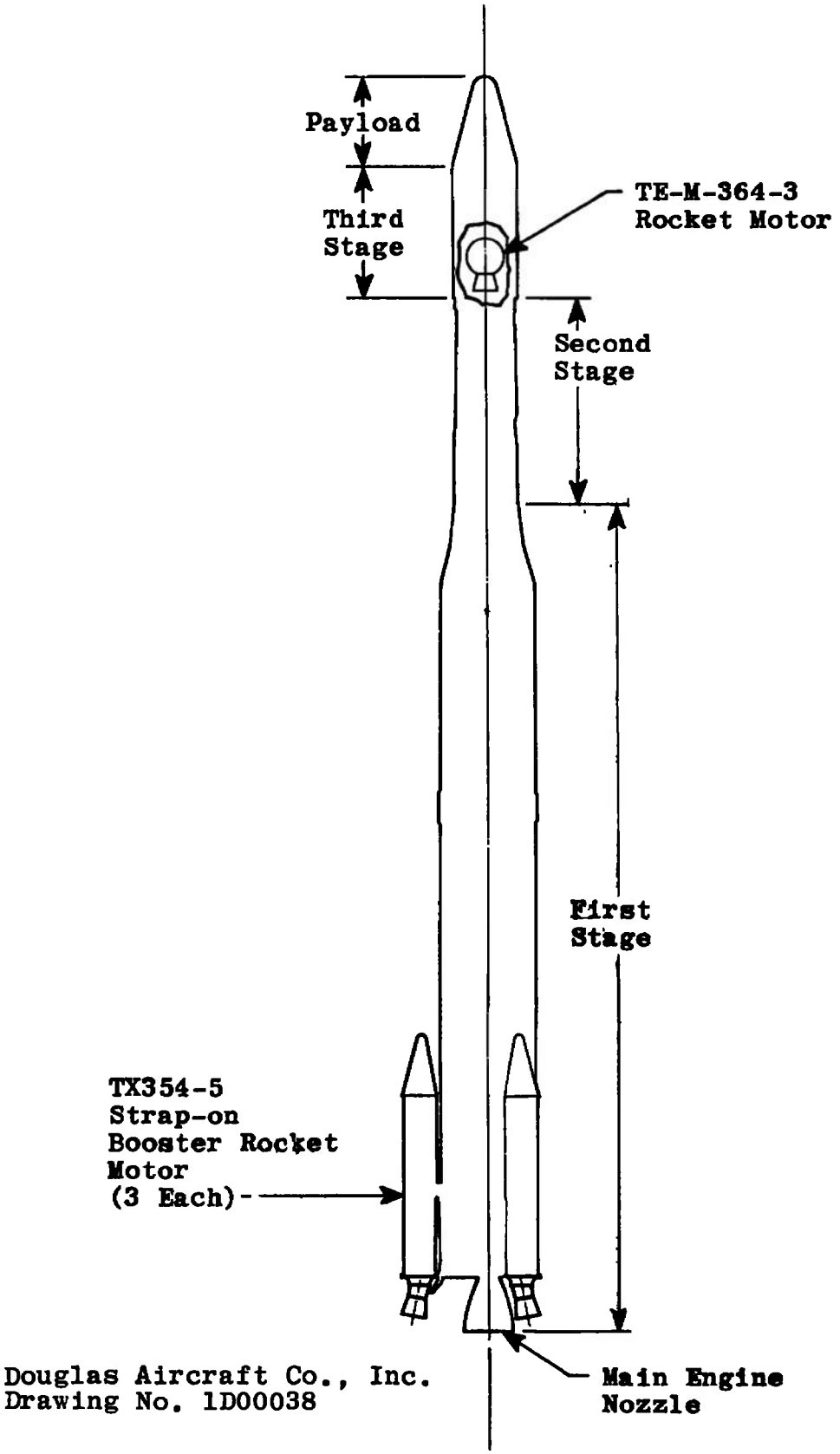

Fig. 1 Schematic of the Improved Delta Launch Vehicle DSV-3M

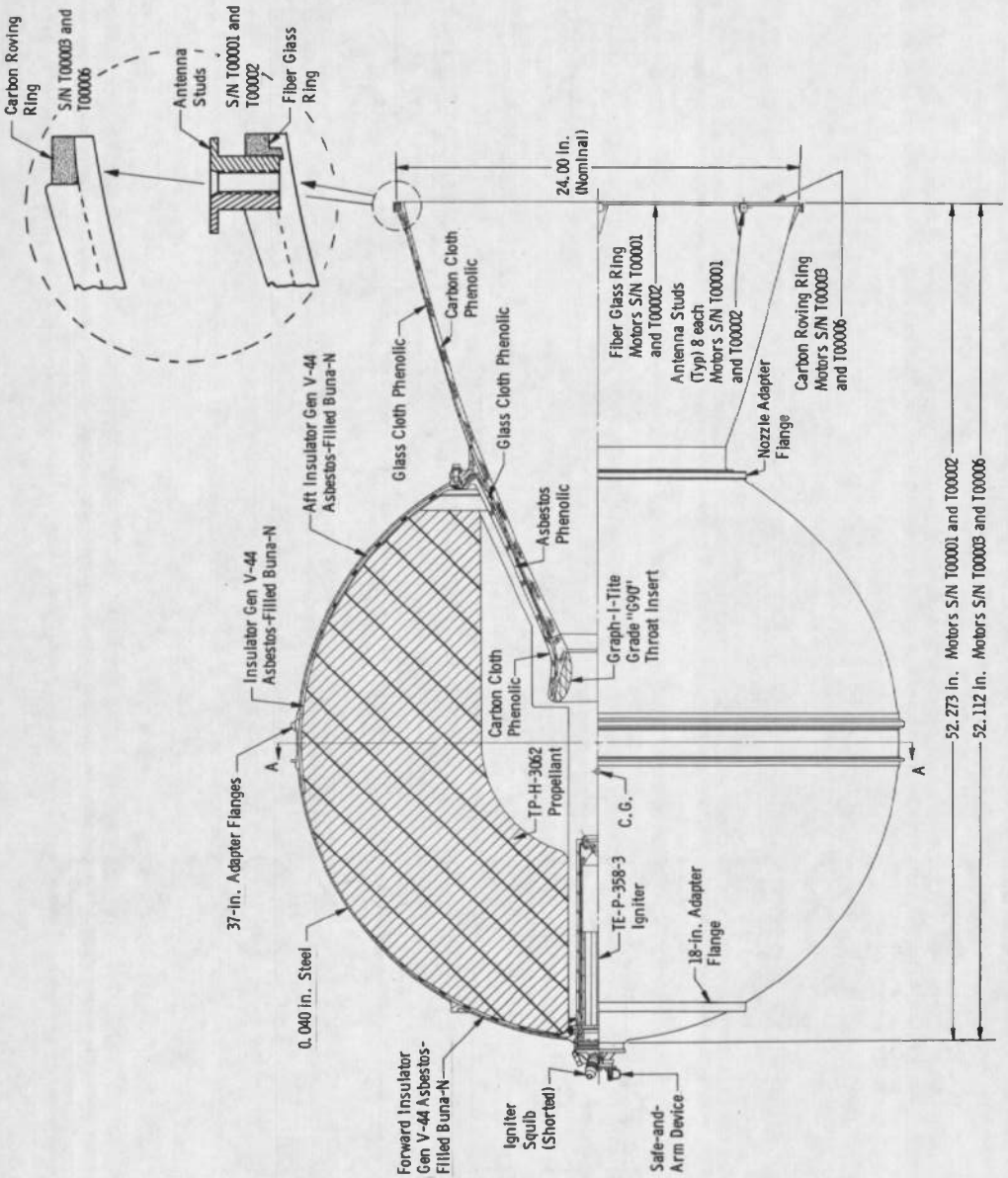

a. Motor Schematic

Fig. 2 TE-M-364-3 Rocket Motor

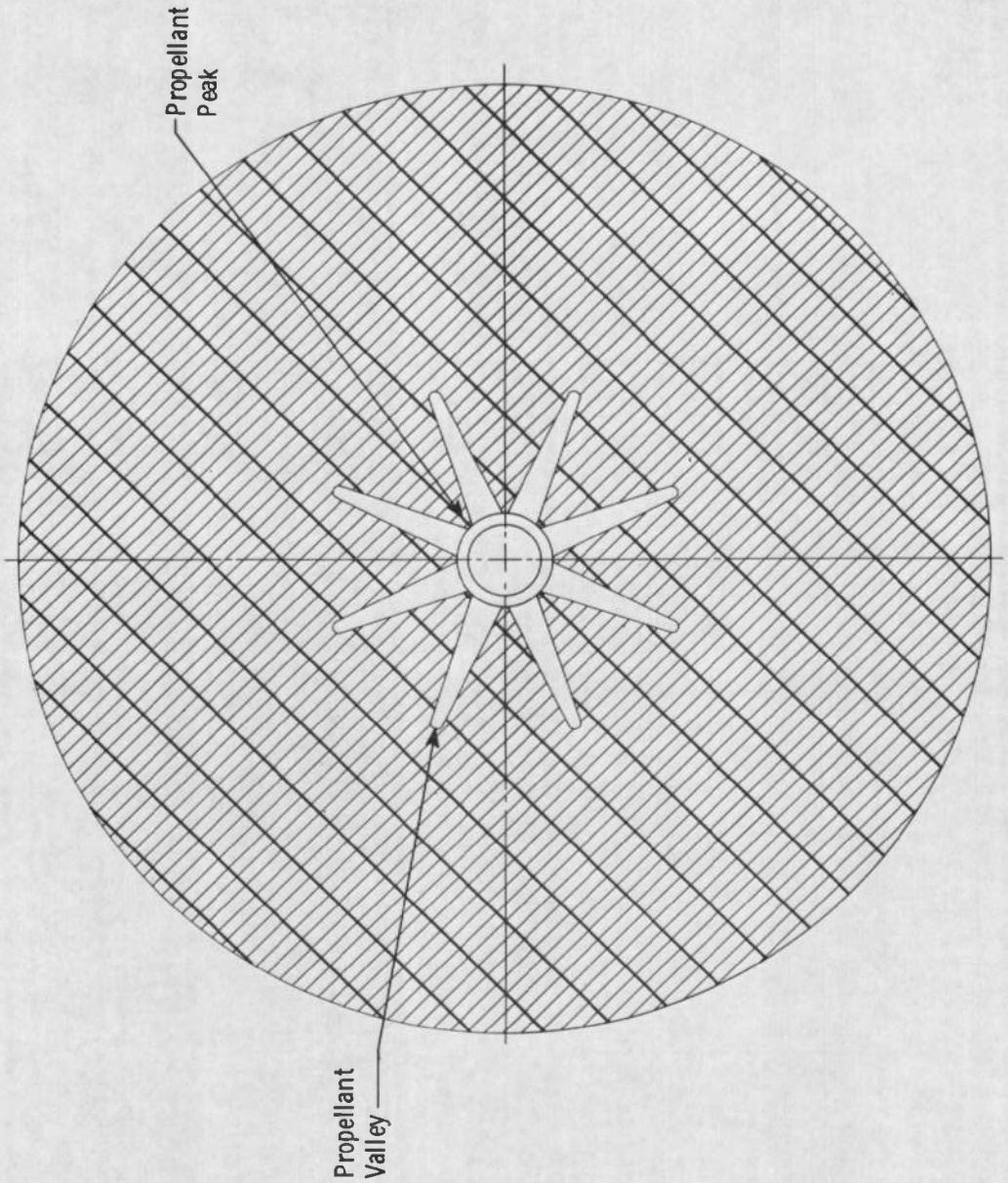

b. Propellant Schematic (Section A-A)

Fig. 2 Continued

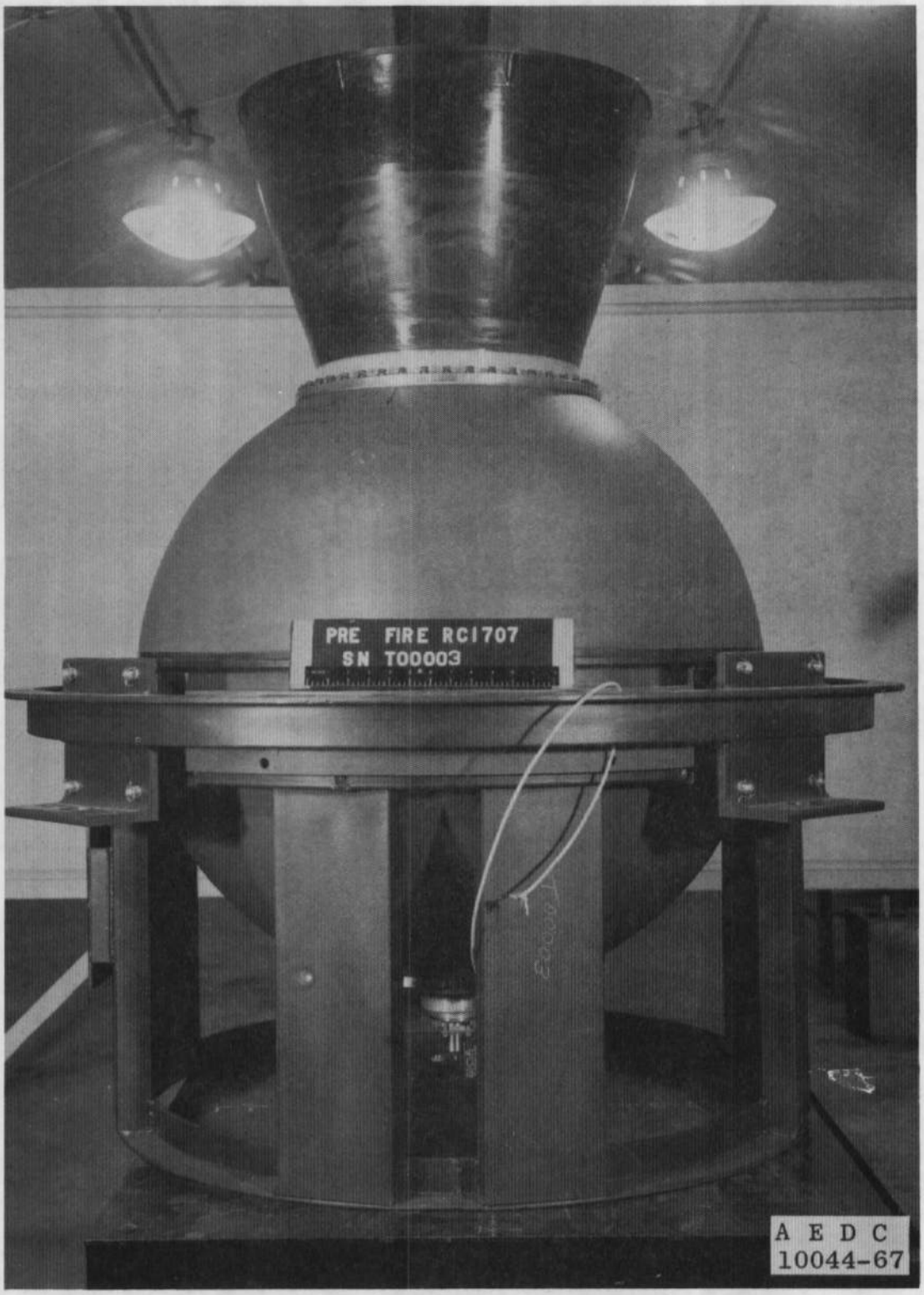

c. Motor Photograph

Fig. 2 Concluded

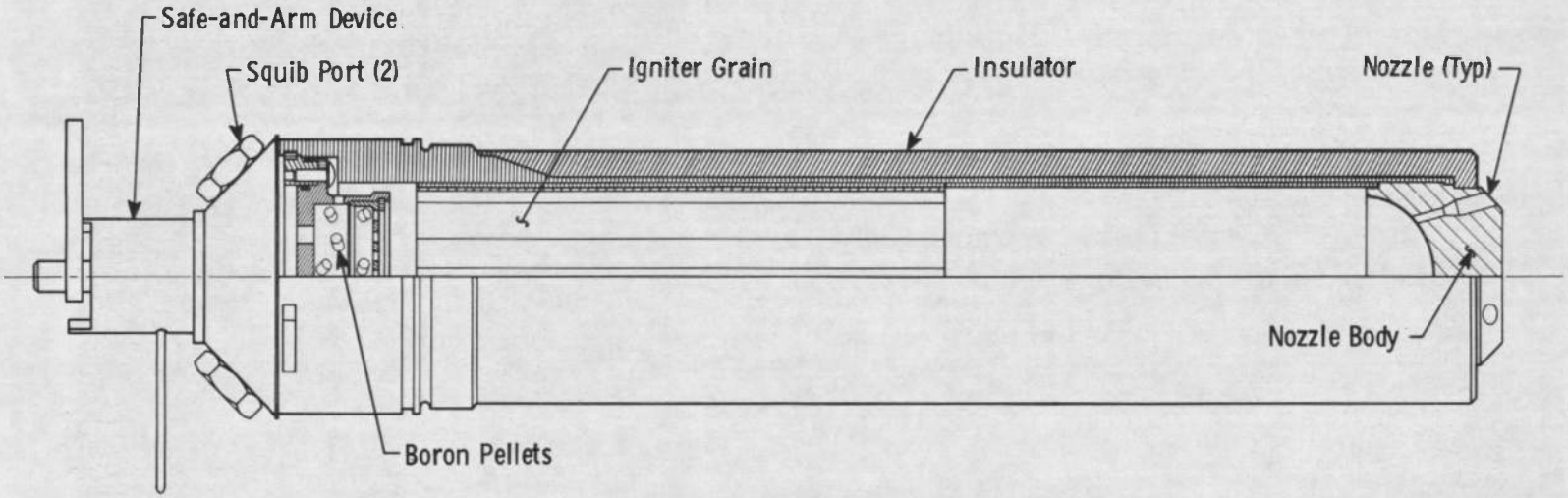

a. Schematic

Fig. 3 TE-P-358-3 Igniter

b. Photograph

Fig. 3 Concluded

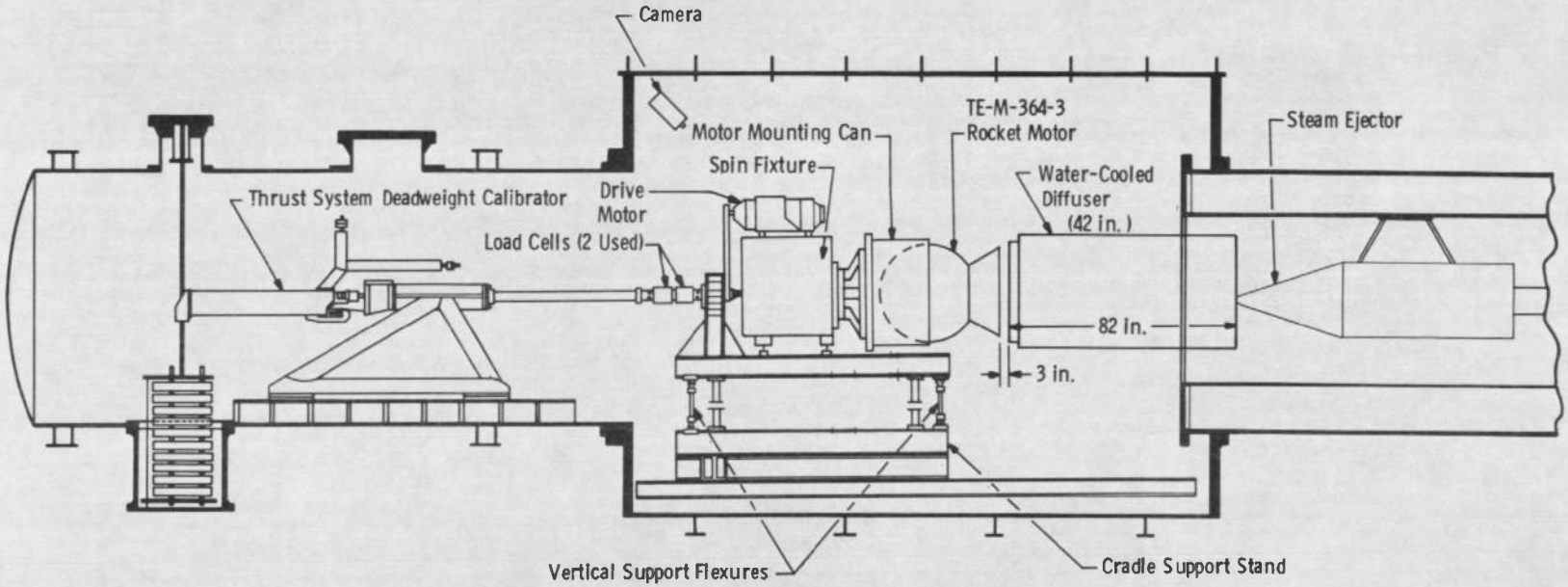

a. Schematic

Fig. 4 Installation of the TE-M-364-3 Motor Assembly in Propulsion Engine Test Cell (T-3)

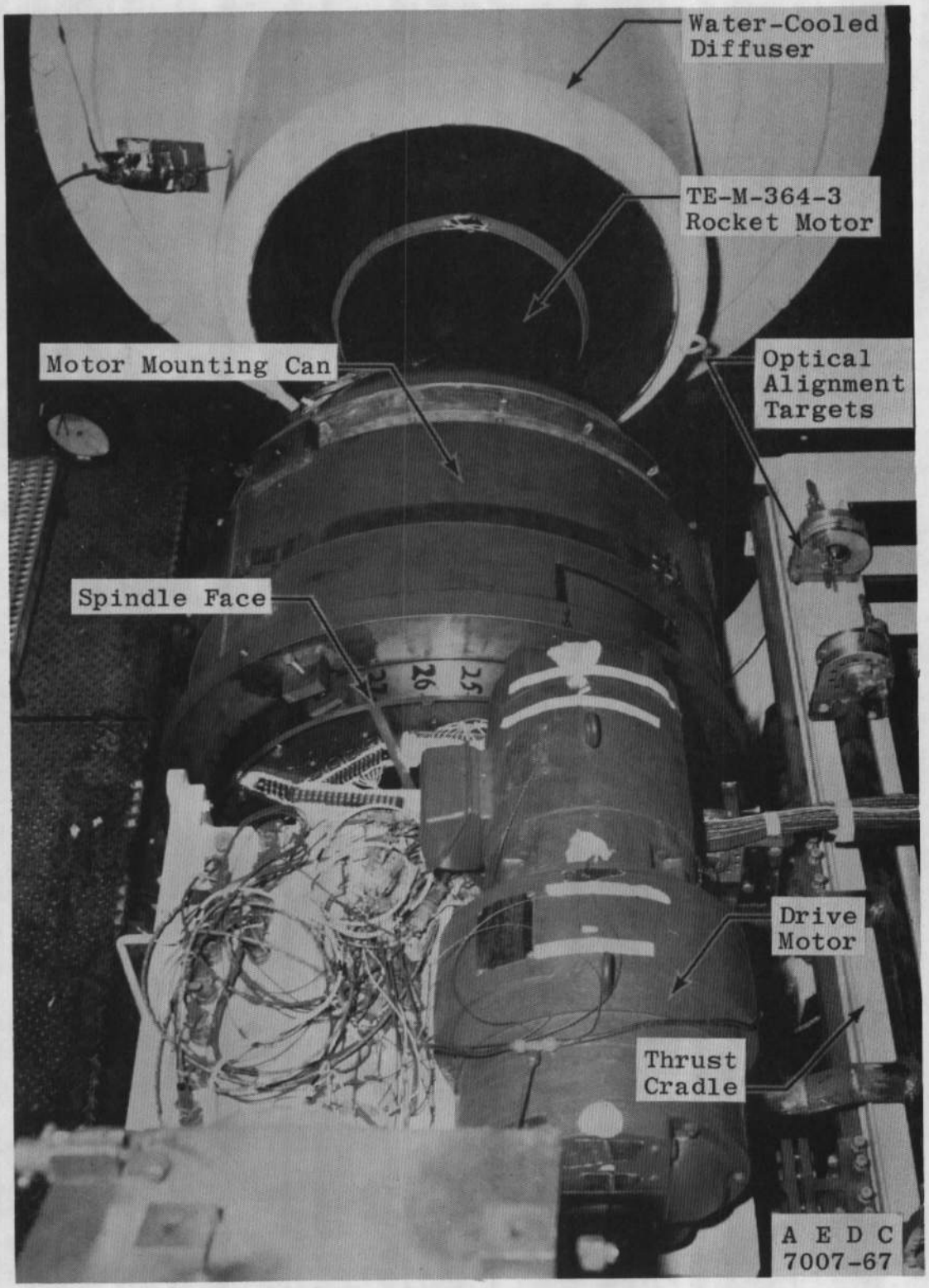

b. Photograph (Looking Downstream)

Fig. 4 Continued

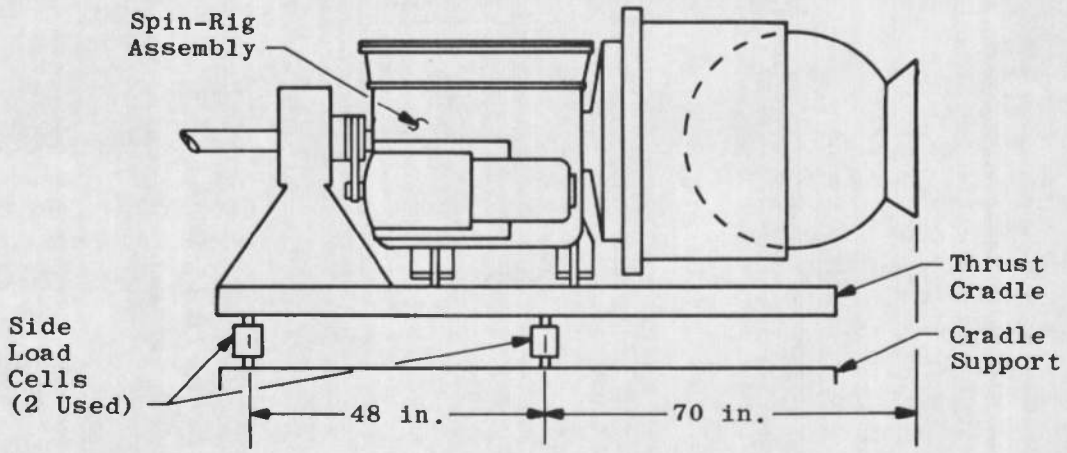

Plan View

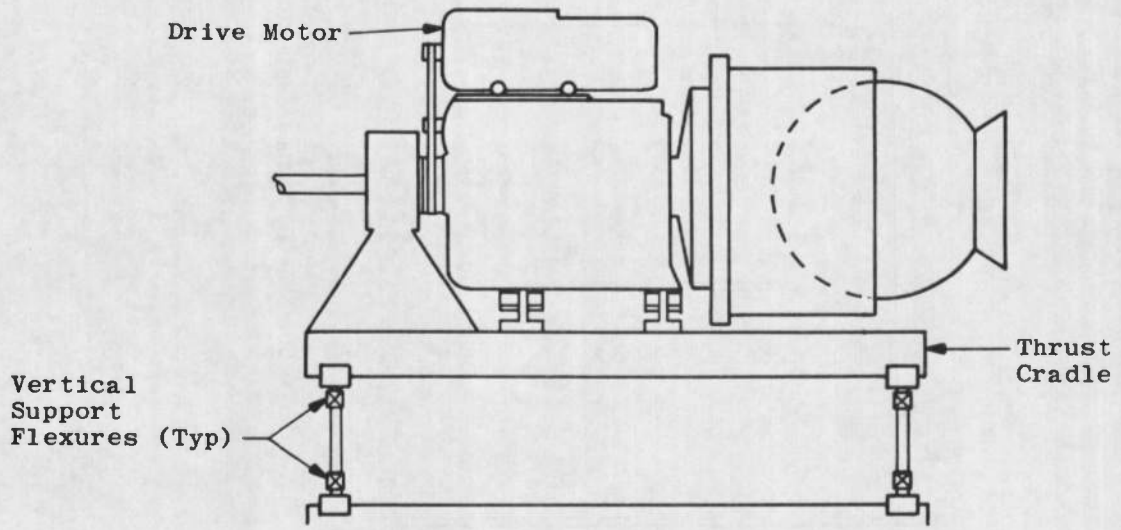

Elevation View

c. Detail

Fig. 4 Concluded

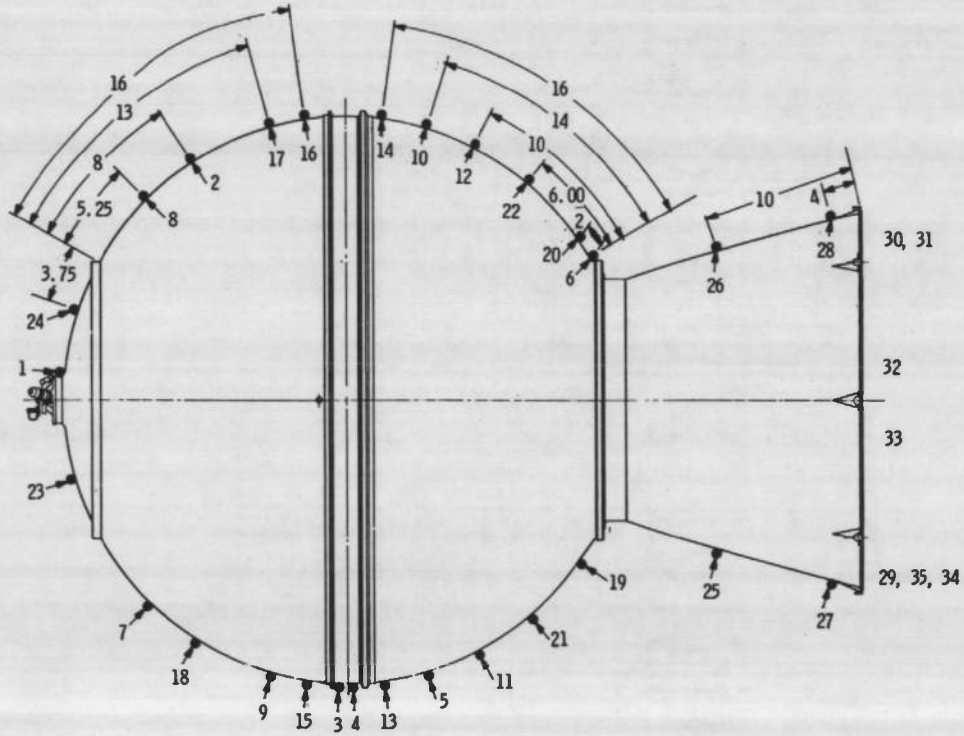

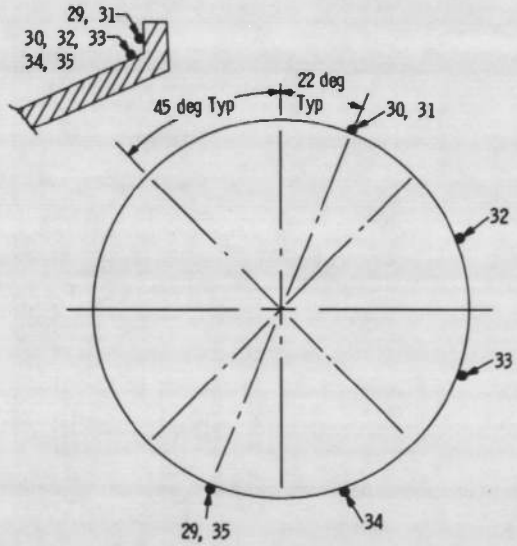

Fig. 5 Schematic Showing Thermocouple Locations on the TE-M-364-3 Motor

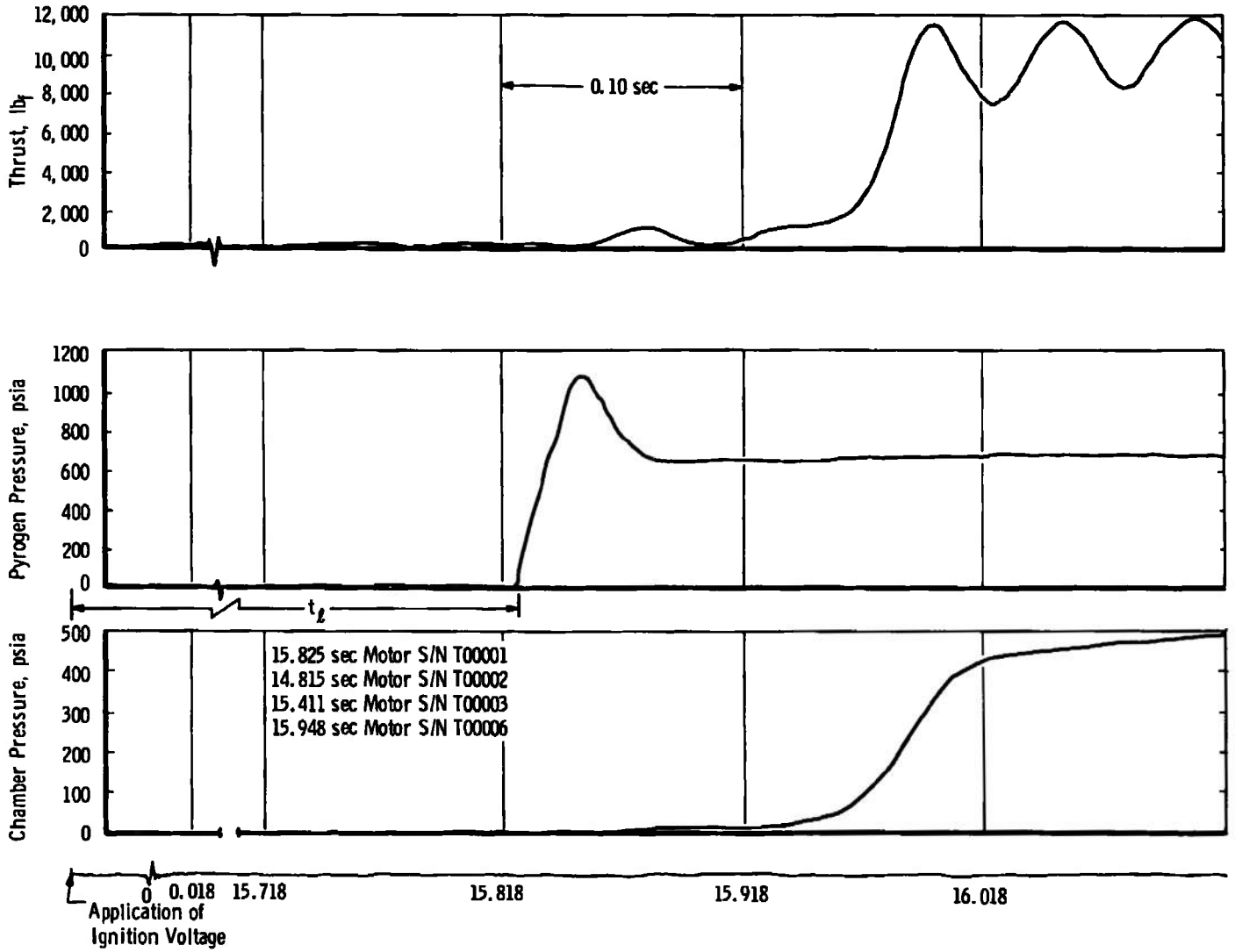

Fig. 6 Analog Trace of Typical Ignition Event

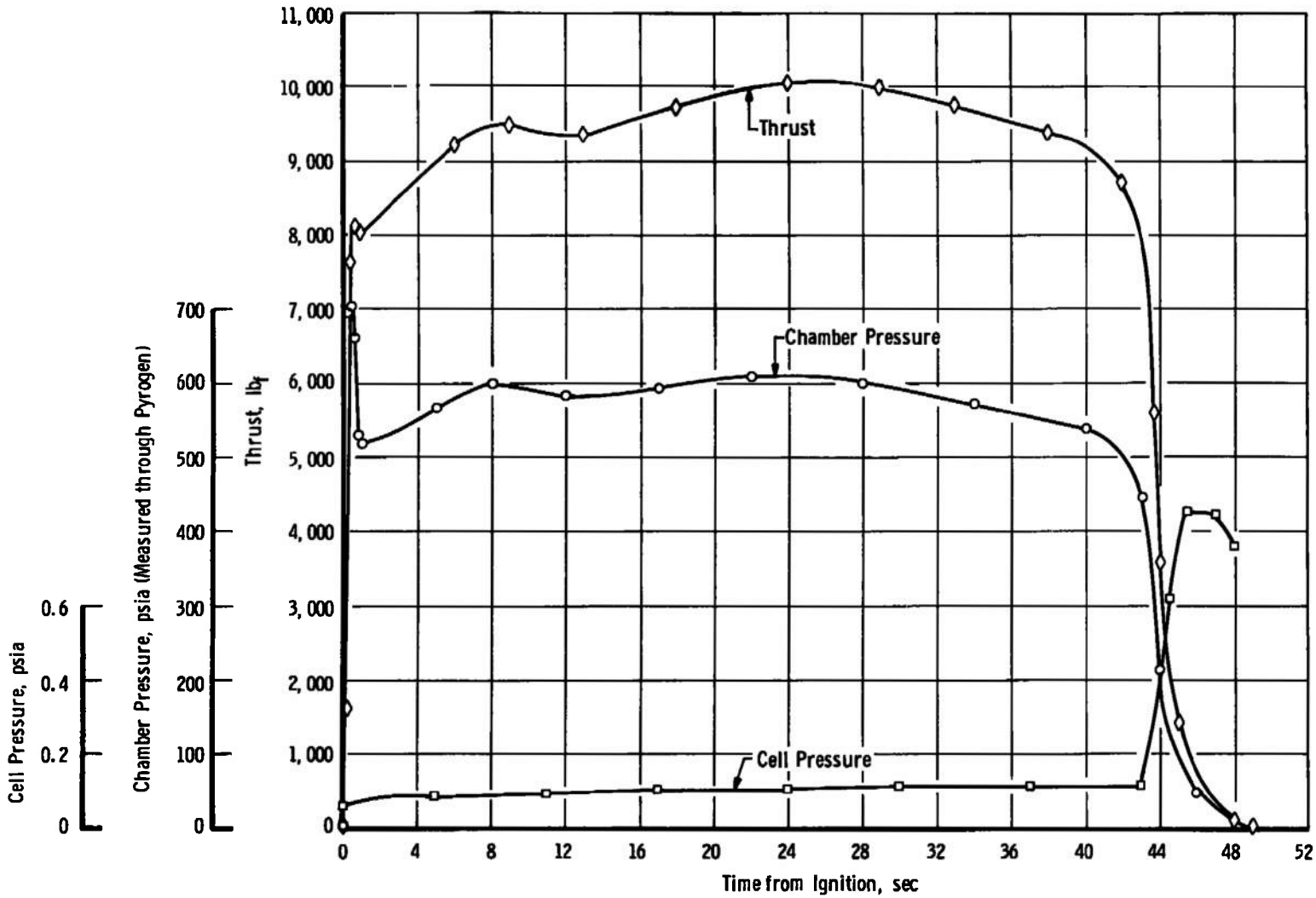

a. Motor S/N T00001 (Spin Mode, 110 rpm; Temperature Conditioned at 55 ± 5°F)

Fig. 7 Variations of Thrust, Chamber Pressure, and Test Cell Pressure during Motor Burn Time

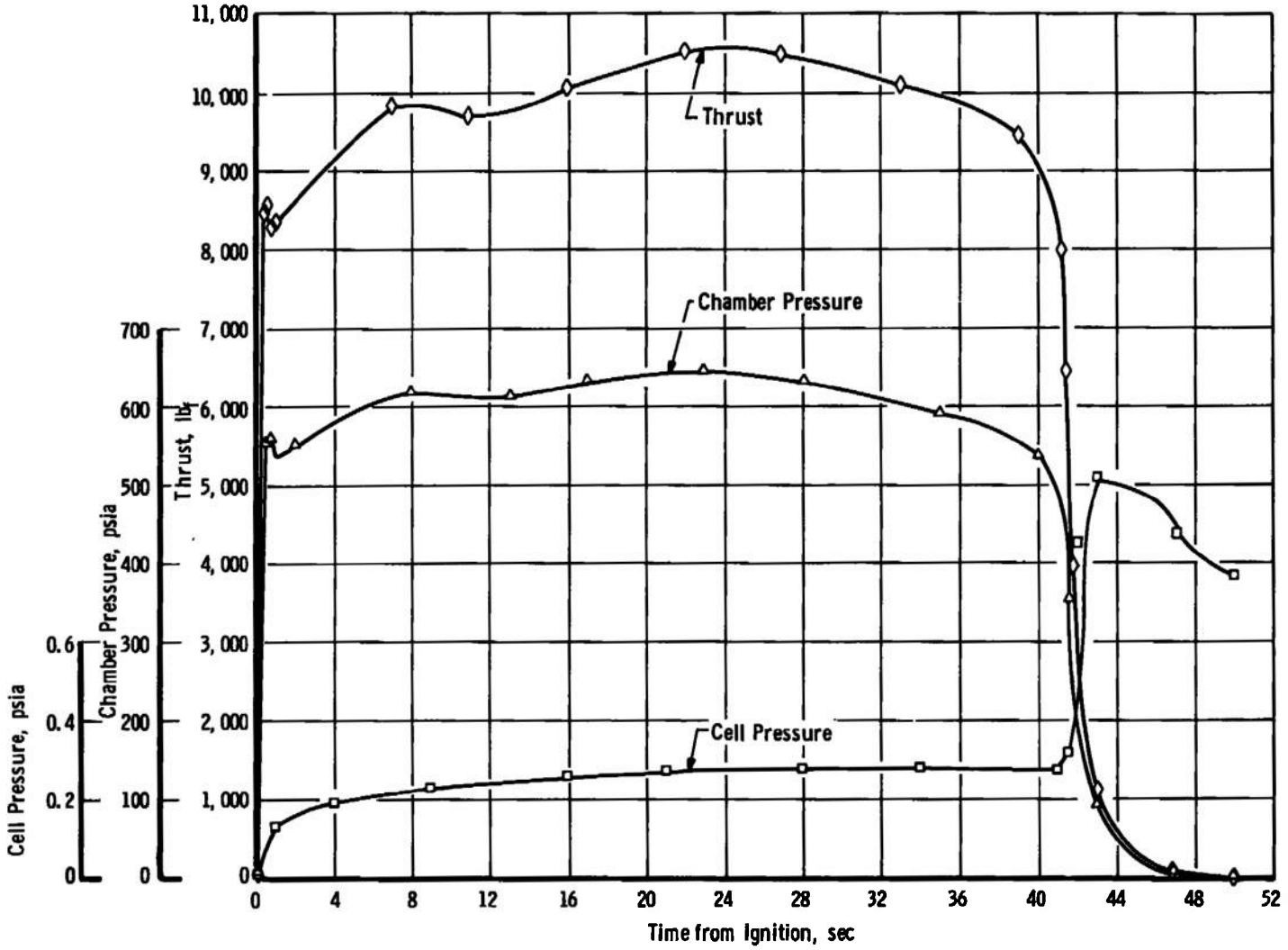

b. Motor S/N T00002 (Spin Mode, 110 rpm; Temperature Conditioned at 95 ± 5°F)

Fig. 7 Continued

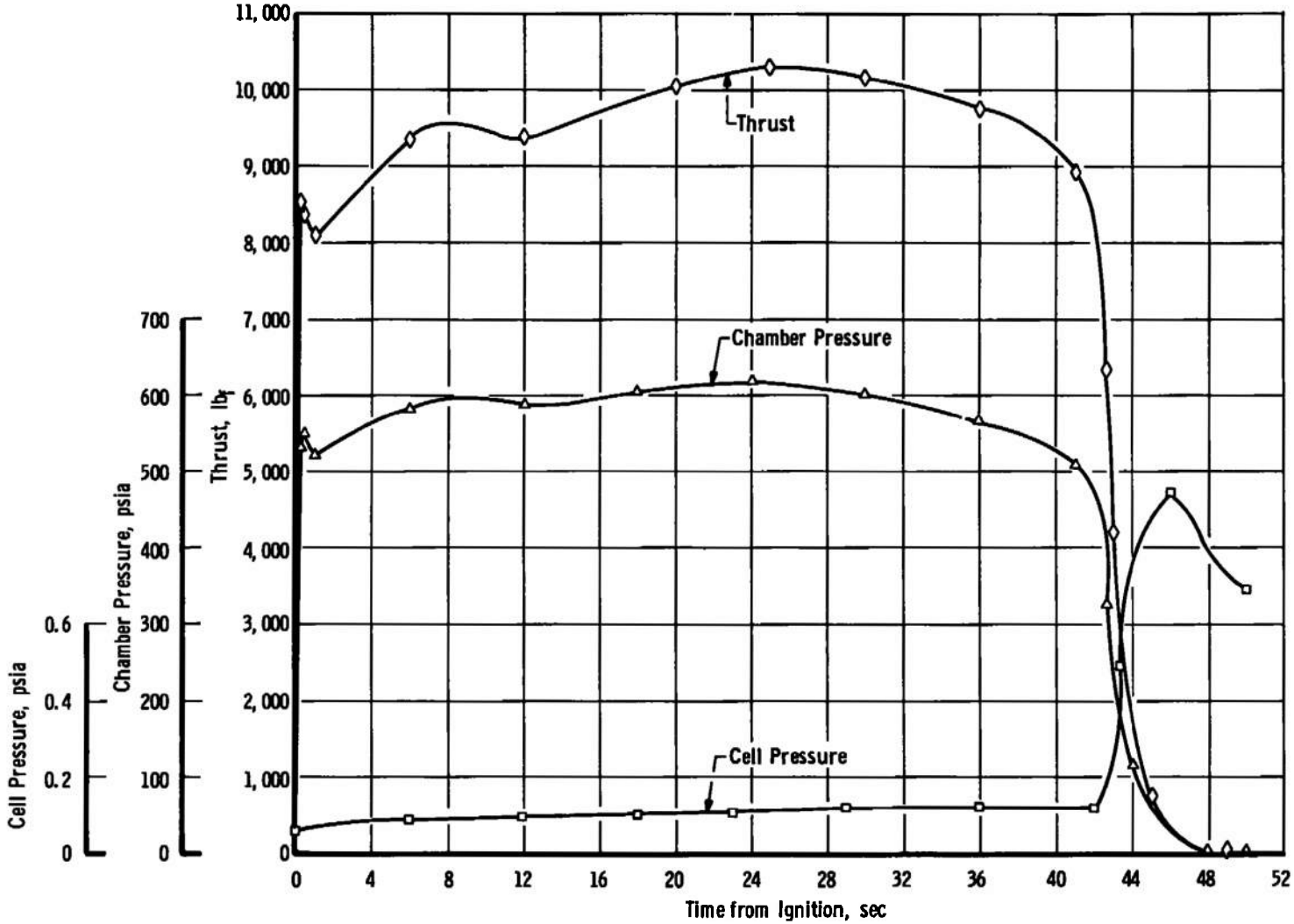

c. Motor S/N T00003 (No-Spin Mode; Temperature Conditioned at 75 ± 5°F)

Fig. 7 Continued

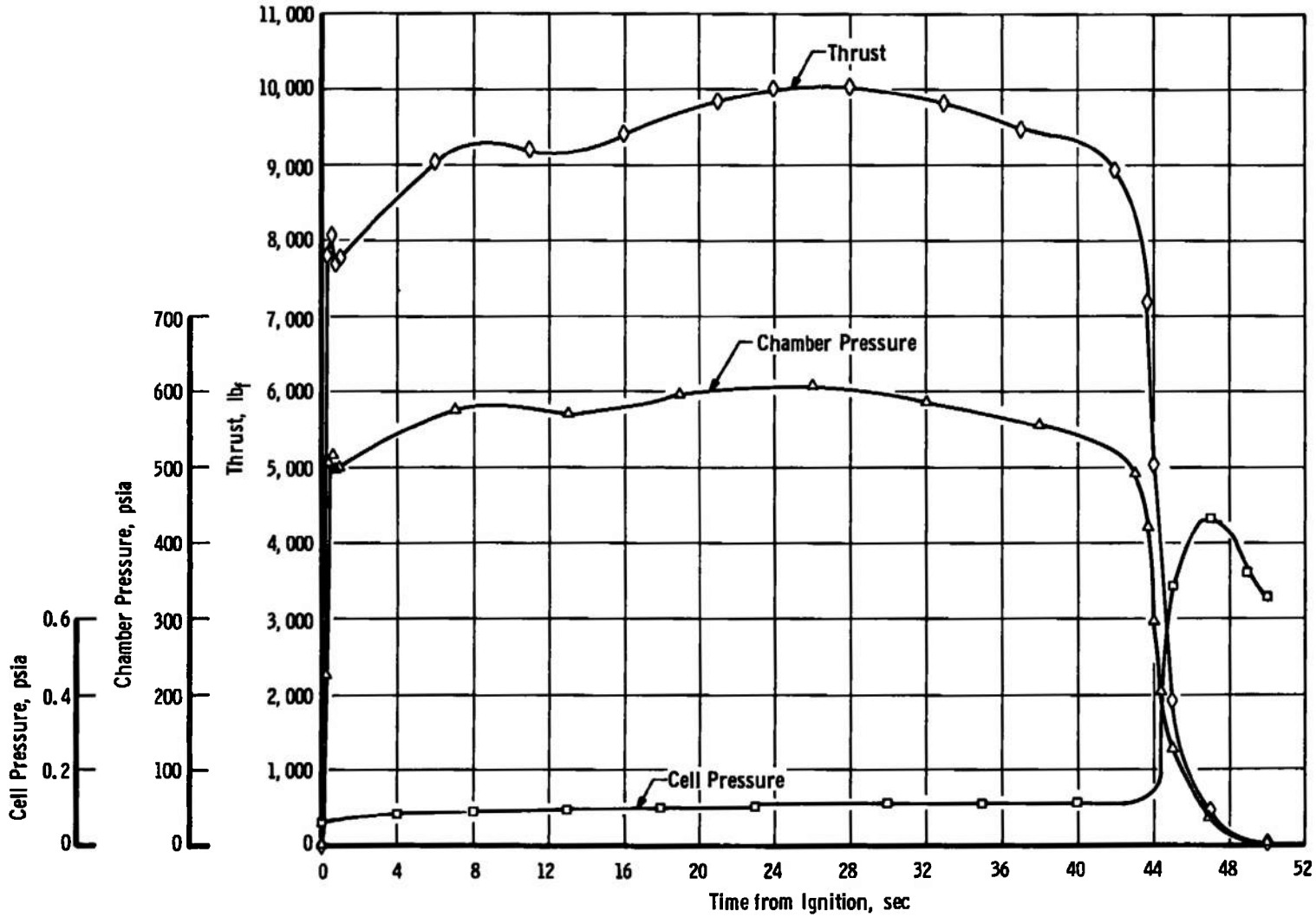

d. Motor S/N T00006 (Spin Mode, 110 rpm; Temperature Conditioned at 50 ± 5°F)

Fig. 7 Concluded

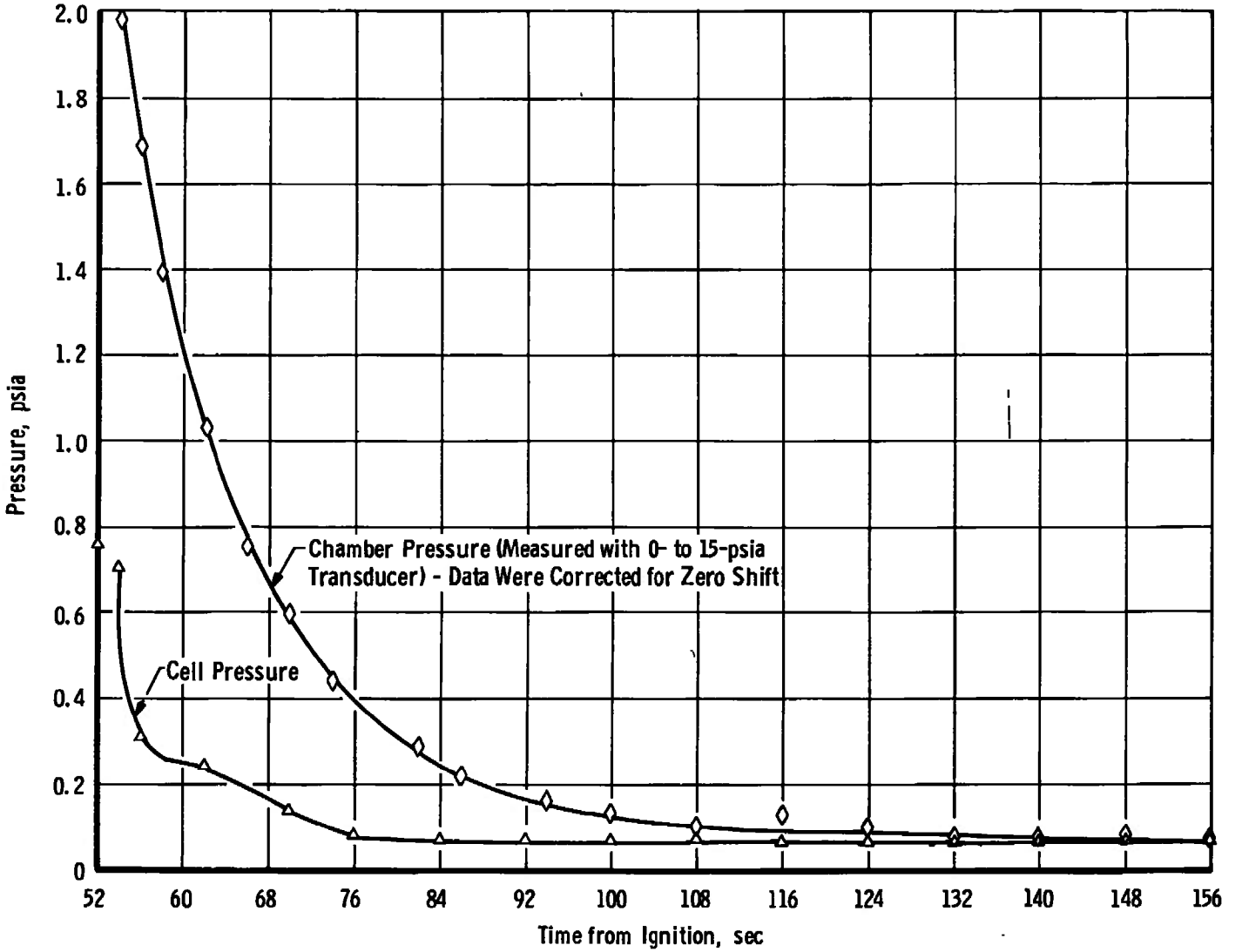

o. Motor S/N T00001 (Spin Mode, 110 rpm)

Fig. 8 Comparison of Low-Range Chamber Pressure and Test Cell Pressure during Motor Tailoff

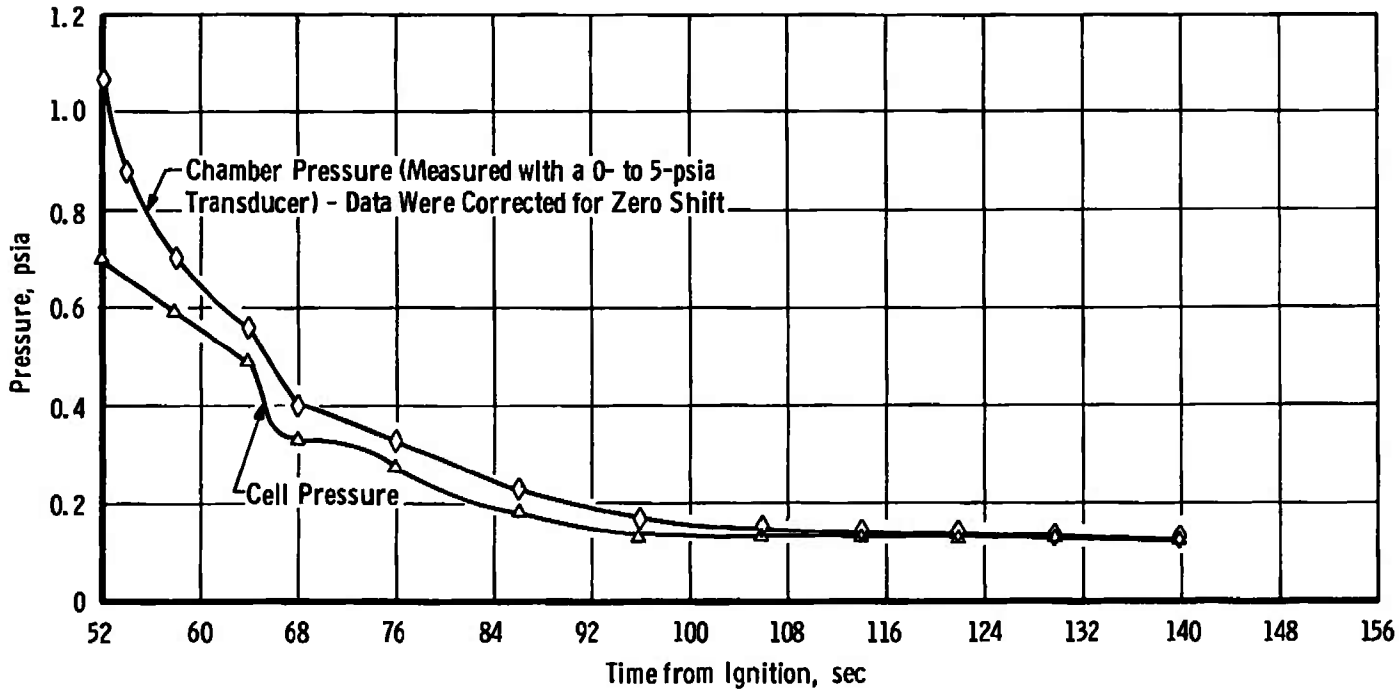

Fig. 8b b. Motor S/N T00002 (Spin Mode, 110 rpm)

Fig. 8 Continued

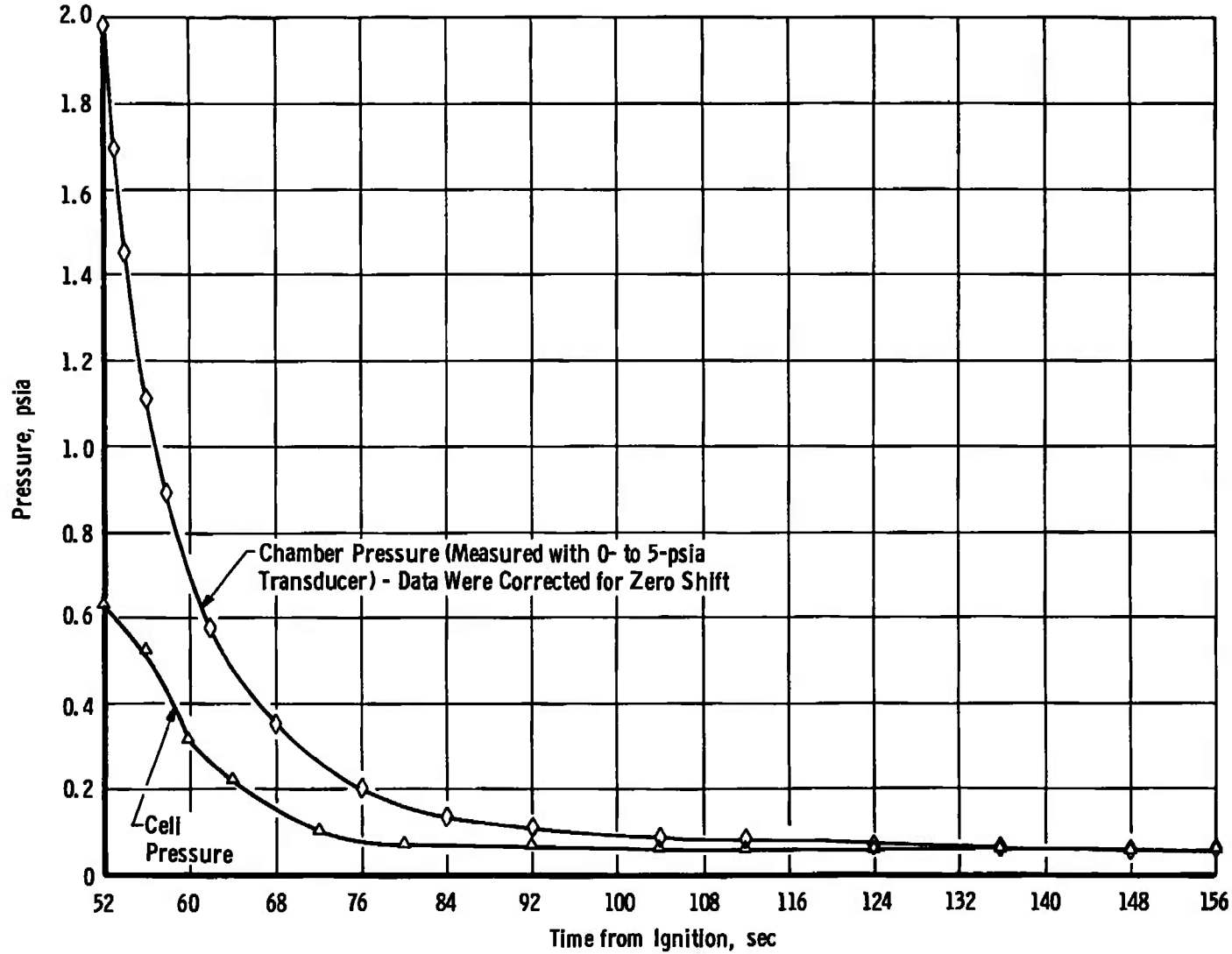

c. Motor S/N T00003 (No-Spin Mode)

Fig. 8 Continued

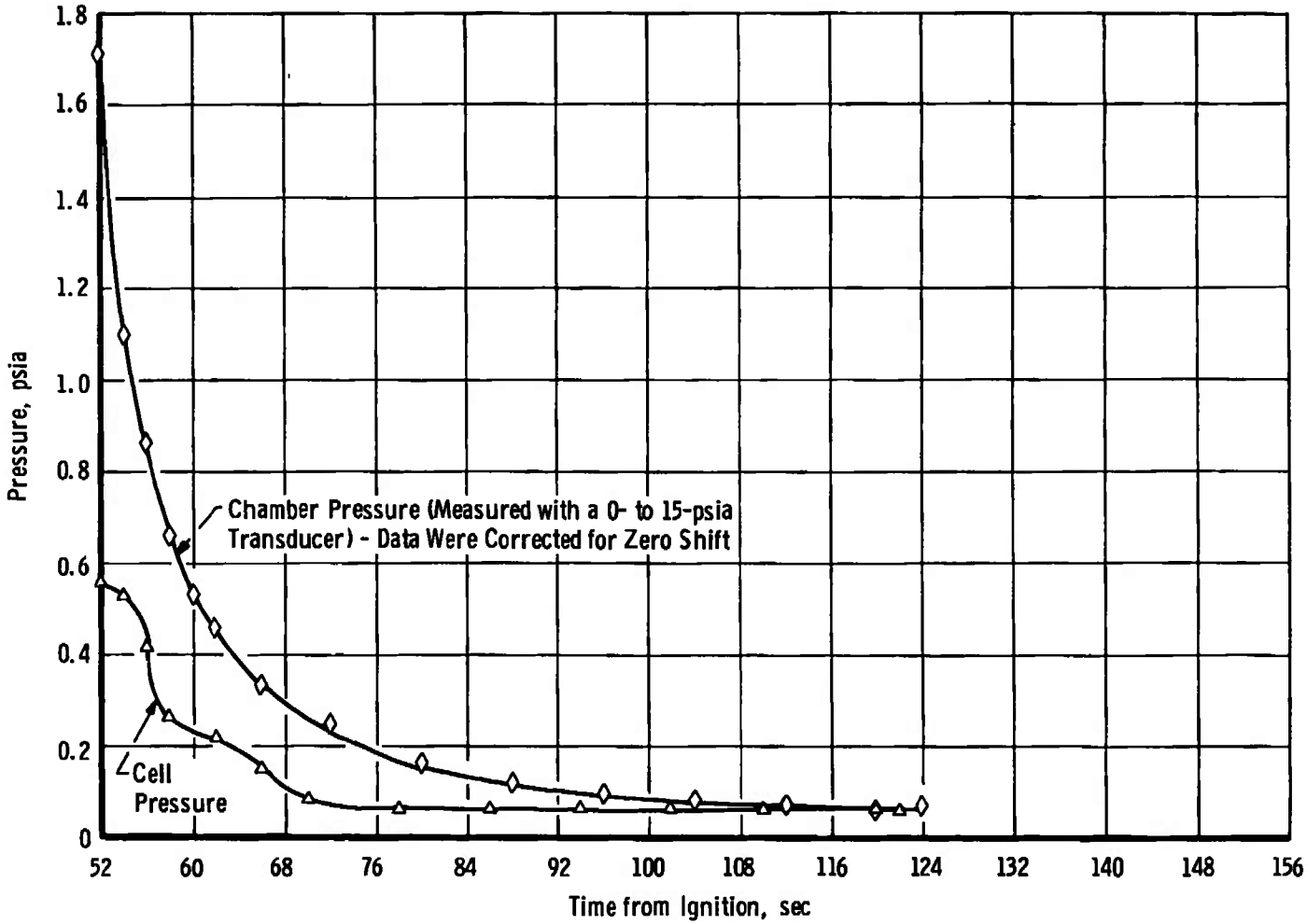

d. Motor S/N T00006 (Spin Mode, 110 rpm)

Fig. 8 Concluded

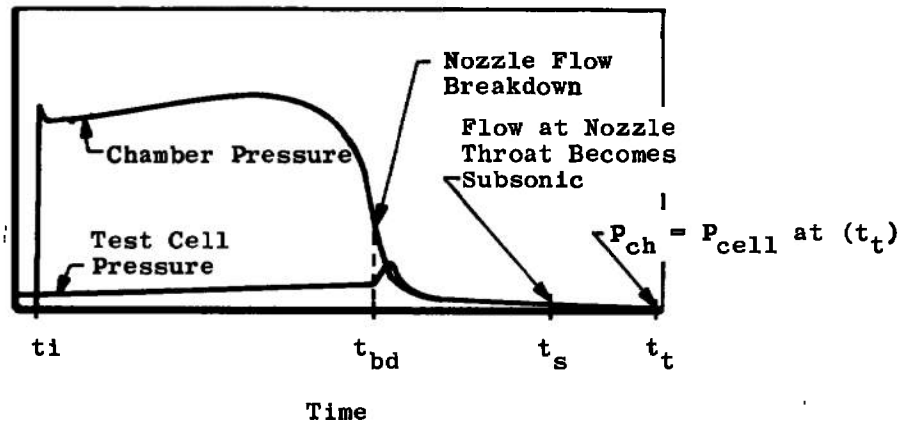

$$I_{vac} = \int_{ti}^{t_{bd}} Fdt + A_{ex_{avg}} \int_{ti}^{t_{bd}} P_{cell}dt + \bar{c}_F A_{t_{post\text{-}fire}} \int_{t_{bd}}^{t_s} P_{ch}dt$$

$$\int_{ti}^{t_{bd}} Fdt = \begin{cases} 409{,}472 \text{ lb}_f\text{-sec motor S/N T00001} \\ 407{,}161 \text{ lb}_f\text{-sec motor S/N T00002} \\ 410{,}277 \text{ lb}_f\text{-sec motor S/N T00003} \\ 409{,}305 \text{ lb}_f\text{-sec motor S/N T00006} \end{cases}$$

$$\int_{ti}^{t_{bd}} P_{cell}dt = \begin{cases} 4.5232 \text{ psia-sec motor S/N T00001} \\ 10.302 \text{ psia-sec motor S/N T00002} \\ 4.613 \text{ psia-sec motor S/N T00003} \\ 4.5739 \text{ psia-sec motor S/N T00006} \end{cases}$$

$$\int_{t_{bd}}^{t_s} P_{ch}dt = \begin{cases} 428.80 \text{ psia-sec motor S/N T00001} \\ 439.96 \text{ psia-sec motor S/N T00002} \\ 409.34 \text{ psia-sec motor S/N T00003} \\ 392.60 \text{ psia-sec motor S/N T00006} \end{cases}$$

$$\bar{c}_F = \frac{\int_{t_1}^{t_2} Fdt + A_{ex_{(post)}} \int_{t_1}^{t_2} P_{cell}dt}{A_{t_{post}} \int_{t_1}^{t_2} P_{ch}dt}$$

	S/N T00001	S/N T00002	S/N T00003	S/N T00006
t_1 =	40.55	39.65	39.45	40.55
t_2 =	41.55	40.65	40.45	41.55
$\bar{c}_F$ =	1.848	1.858	1.862	1.859

Fig. 9 Schematic of Chamber and Cell Pressure-Time Variation Defining Characteristic Events

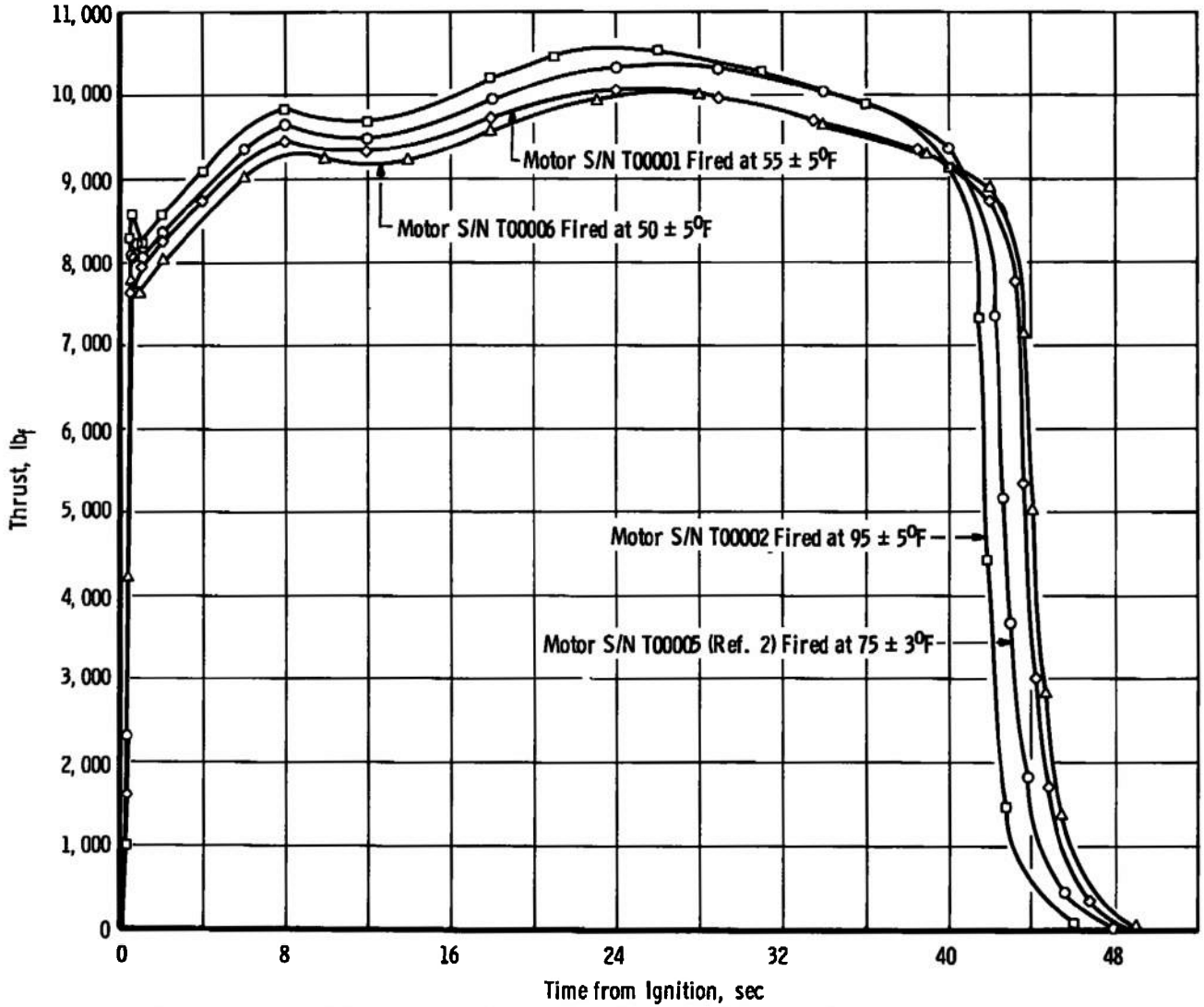

Fig. 10 Comparison of TE-M-364-3 Thrust Variation from the Three Spin Firings Reported Herein and the Ref. 2 Spin Firing

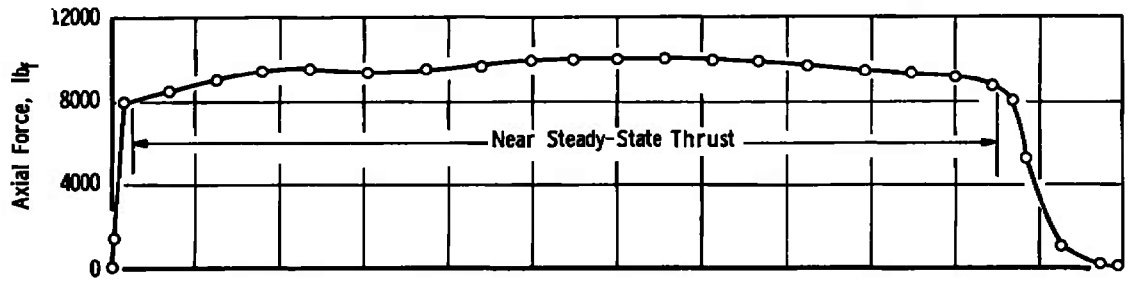

a. Axial Thrust

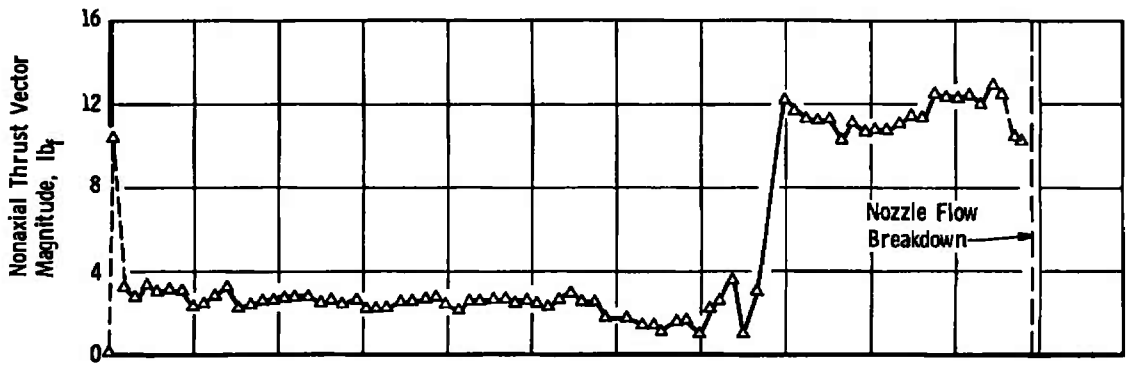

b. Magnitude of Nonaxial Thrust Vector

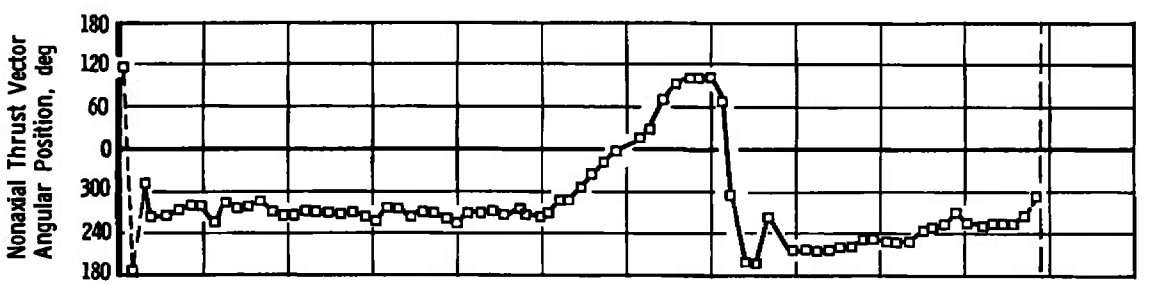

c. Angular Position of Nonaxial Thrust Vector

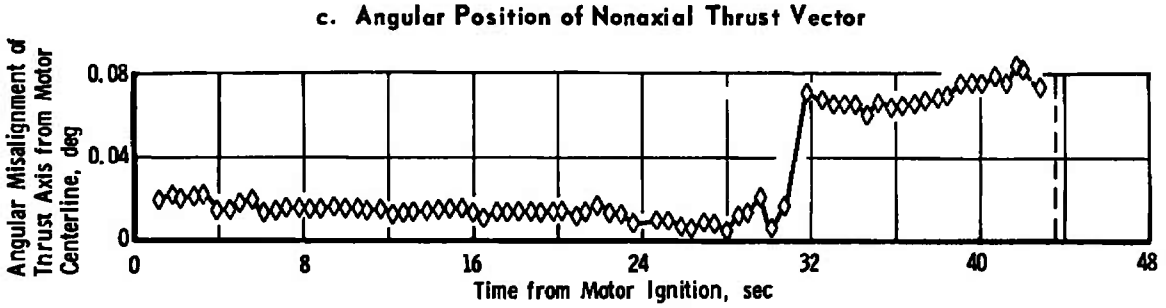

d. Angular Misalignment of Thrust Vector from Motor Centerline

Fig. 11 Nonaxial Thrust Variation with Time for Motor S/N T00001

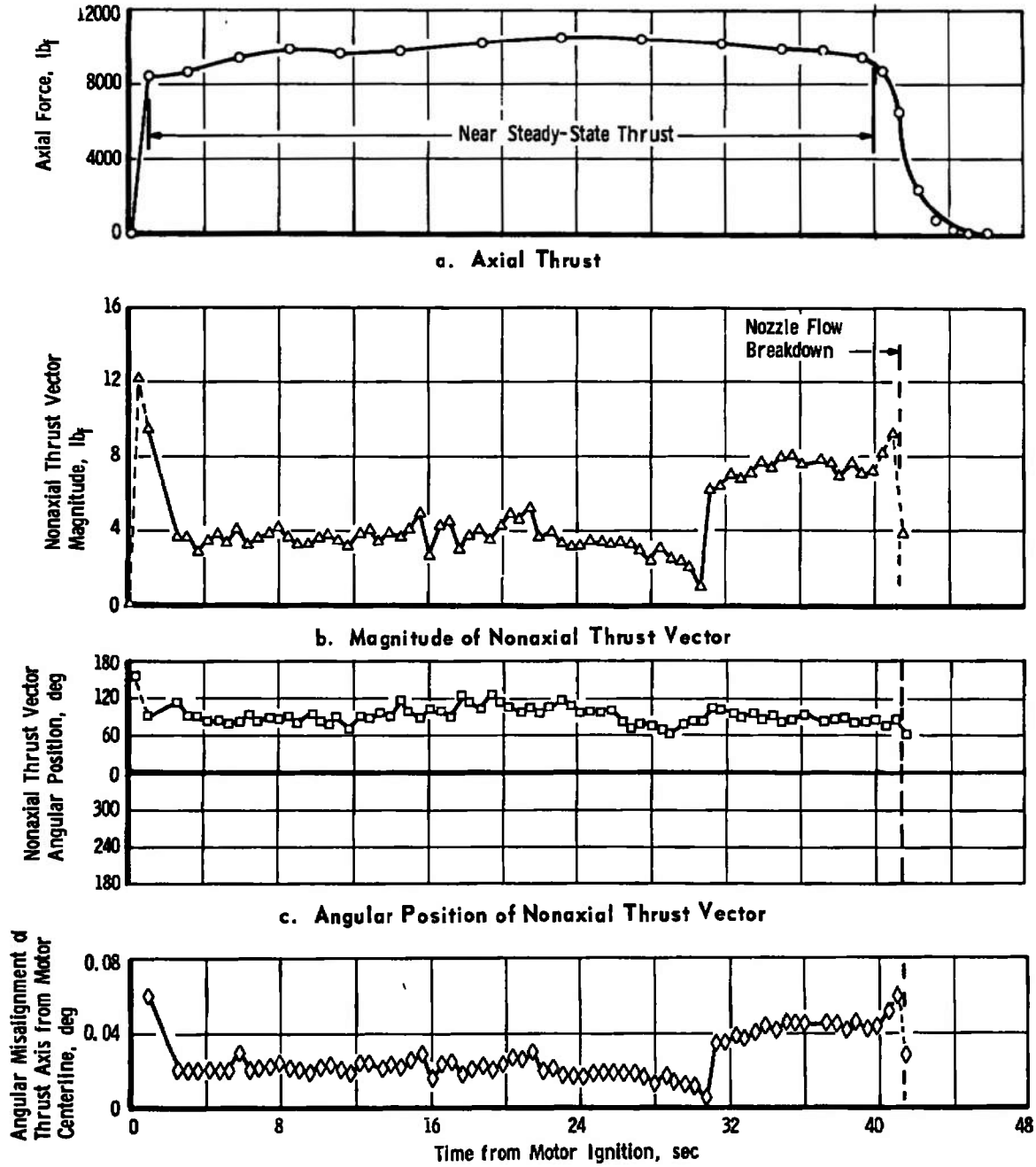

a. Axial Thrust

b. Magnitude of Nonaxial Thrust Vector

c. Angular Position of Nonaxial Thrust Vector

d. Angular Misalignment of Thrust Vector from Motor Centerline

Fig. 12 Nonaxial Thrust Variations with Time for Motor S/N T00002

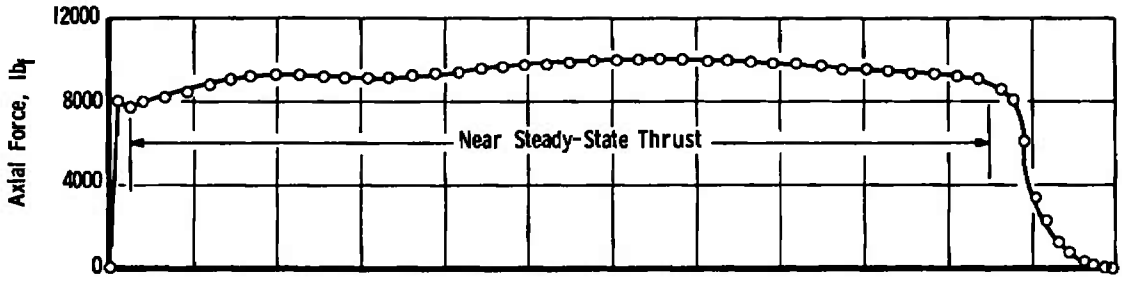

a. Axial Thrust

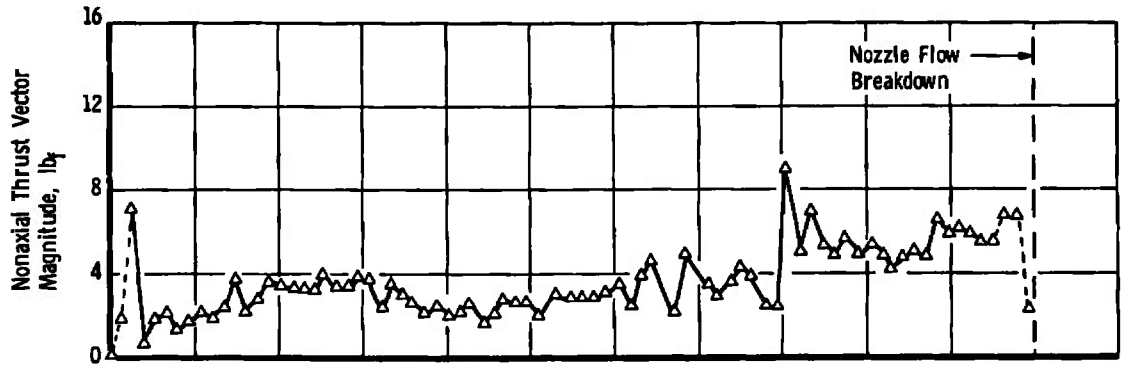

b. Magnitude of Nonaxial Thrust Vector

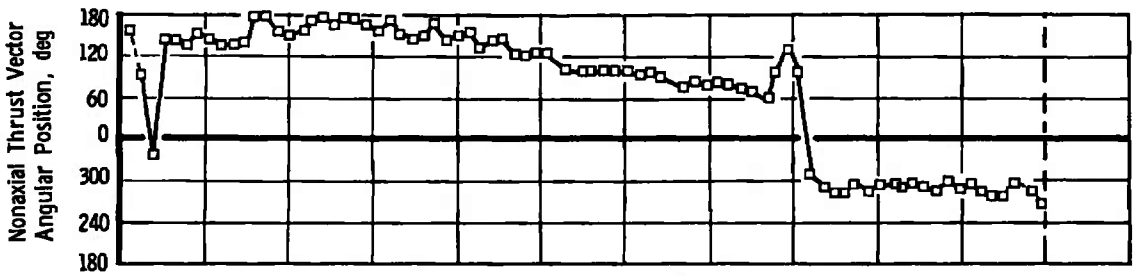

c. Angular Position of Nonaxial Thrust Vector

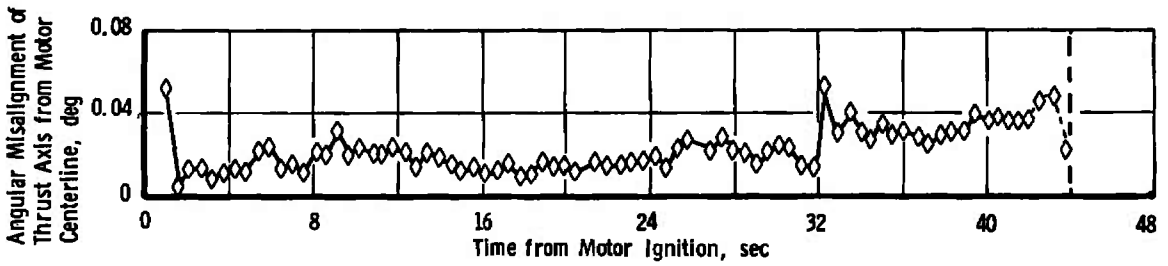

d. Angular Misalignment of Thrust Vector from Motor Centerline

Fig. 13 Nonaxial Thrust Variations with Time for Motor S/N T00006

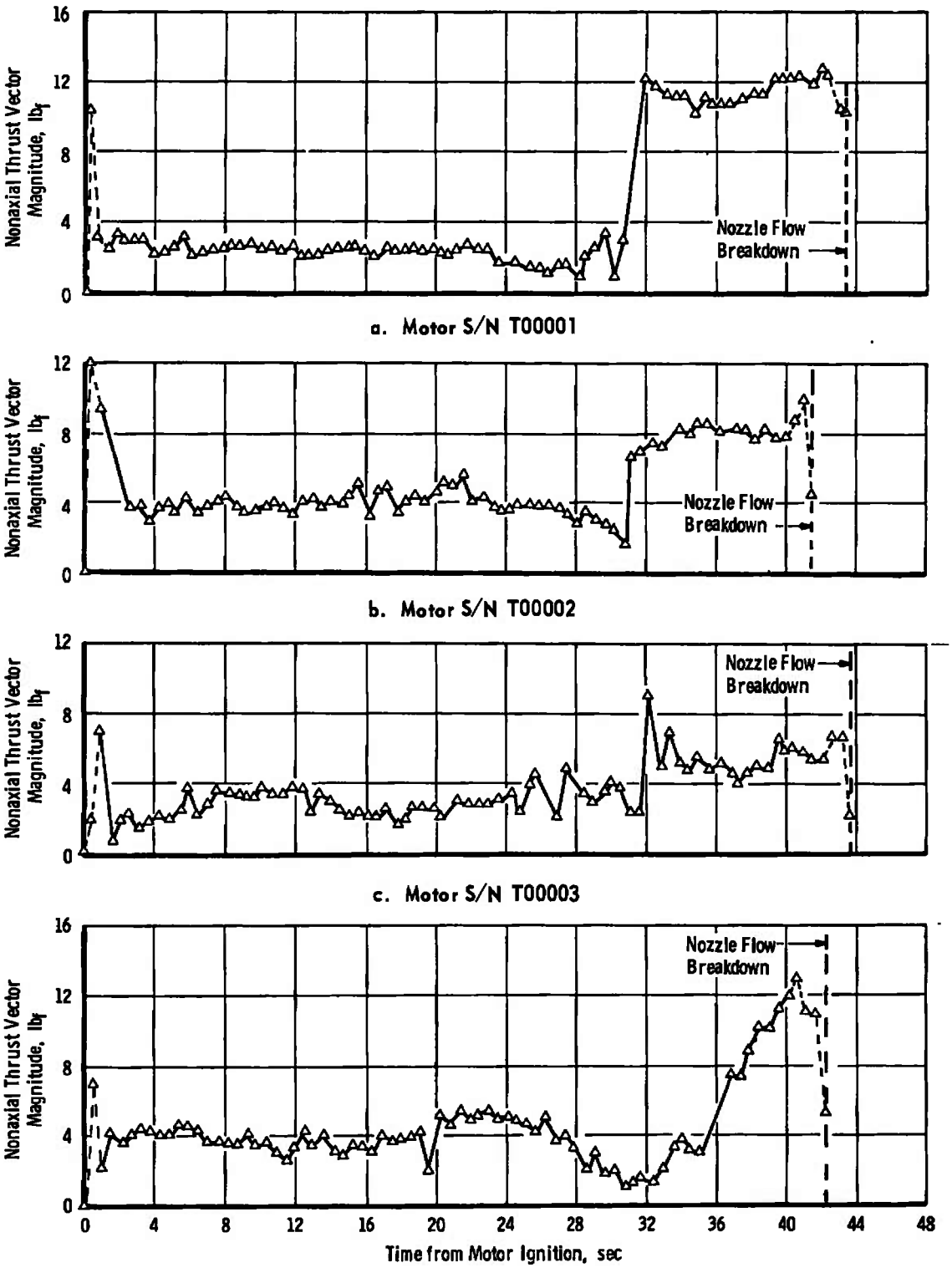

Fig. 14 Comparison of Nonaxial Thrust Vector Magnitude Time Variation for the Three TE-M-364-3 Spin Firings Reported Herein and the One Reported in Ref. 2

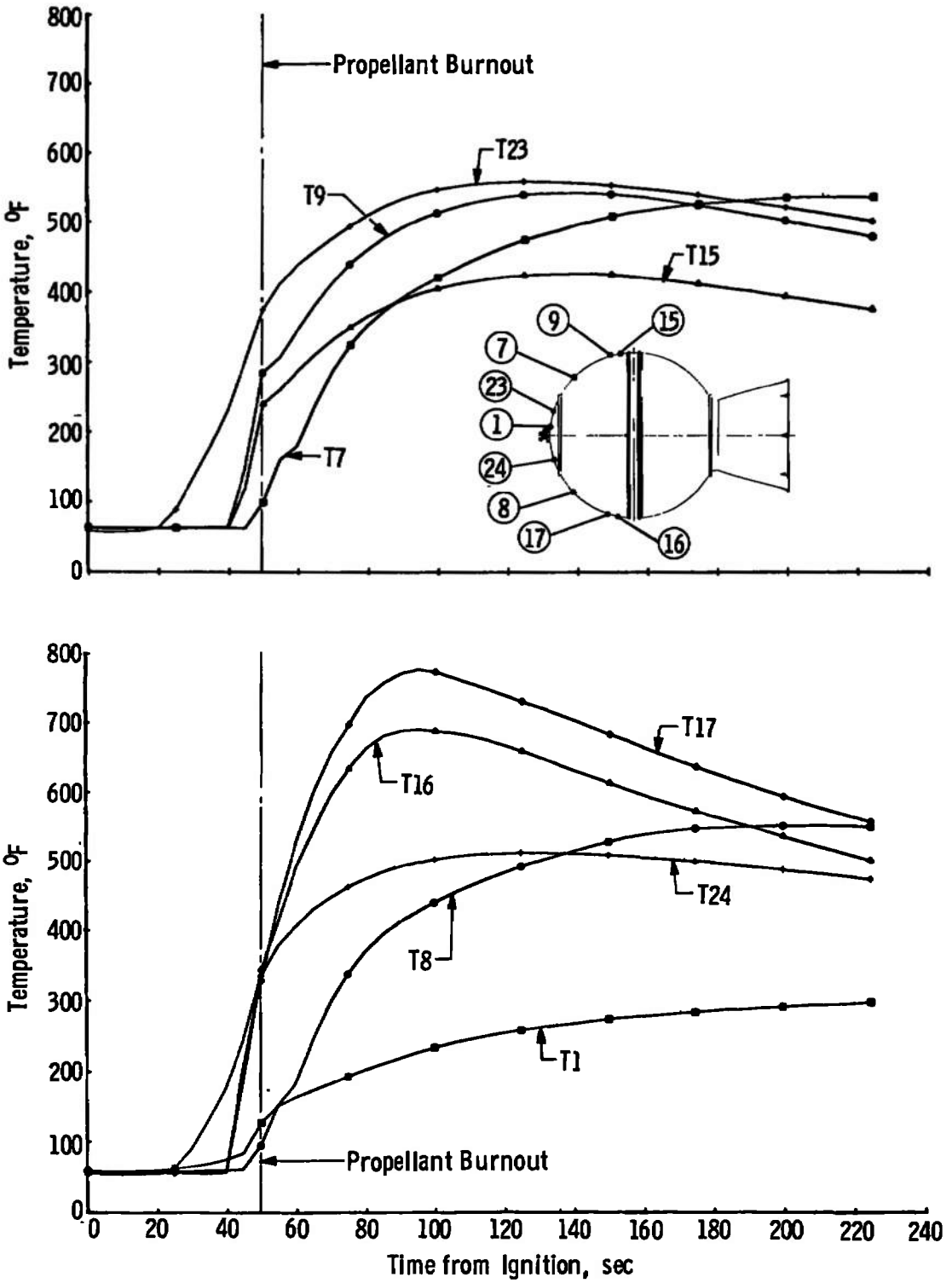

Fig. 15 Time Variation of Typical Motor Case (Forward Hemisphere) Temperatures

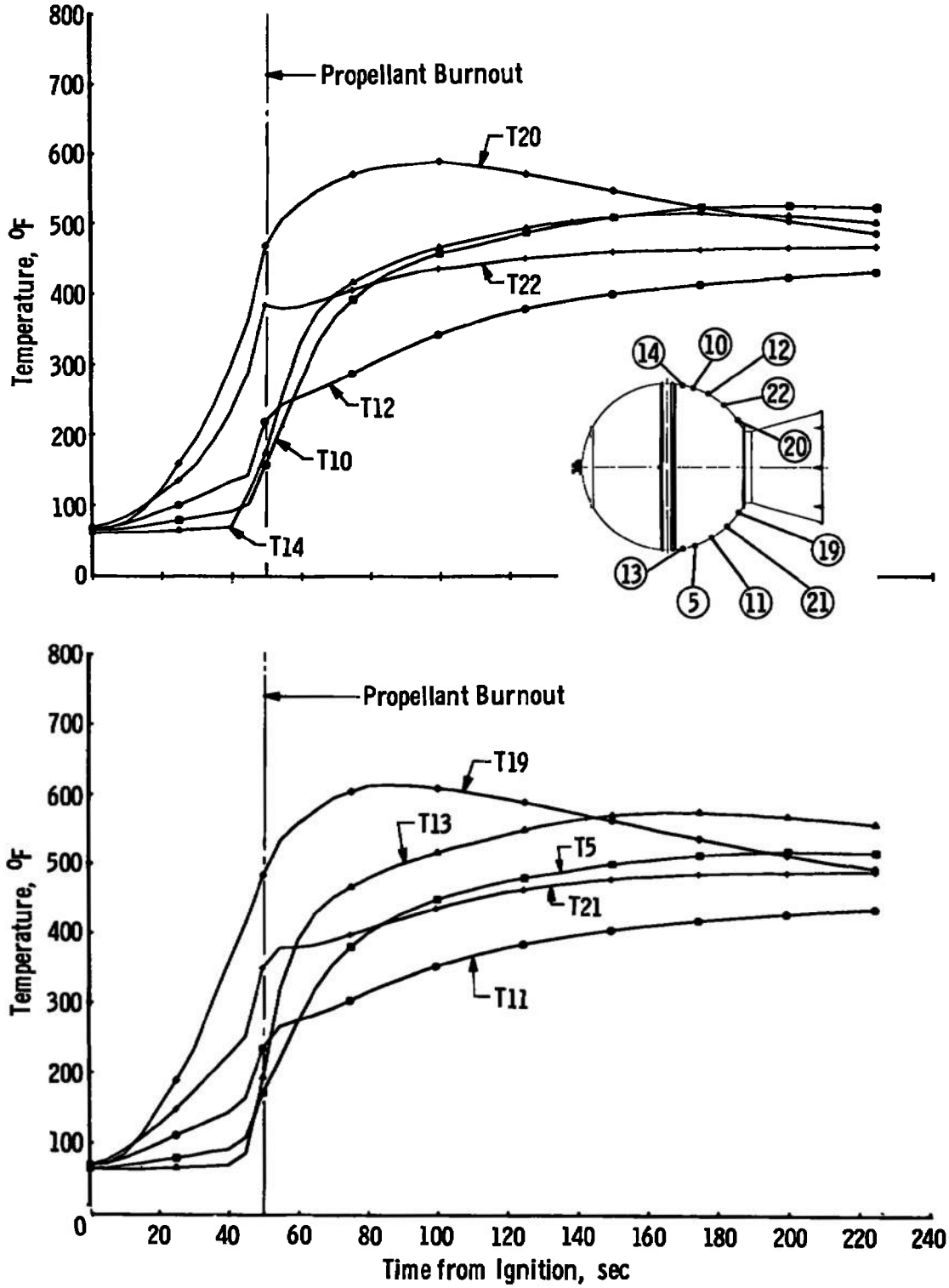

Fig. 16 Time Variation of Typical Motor Case (Aft Hemisphere) Temperatures

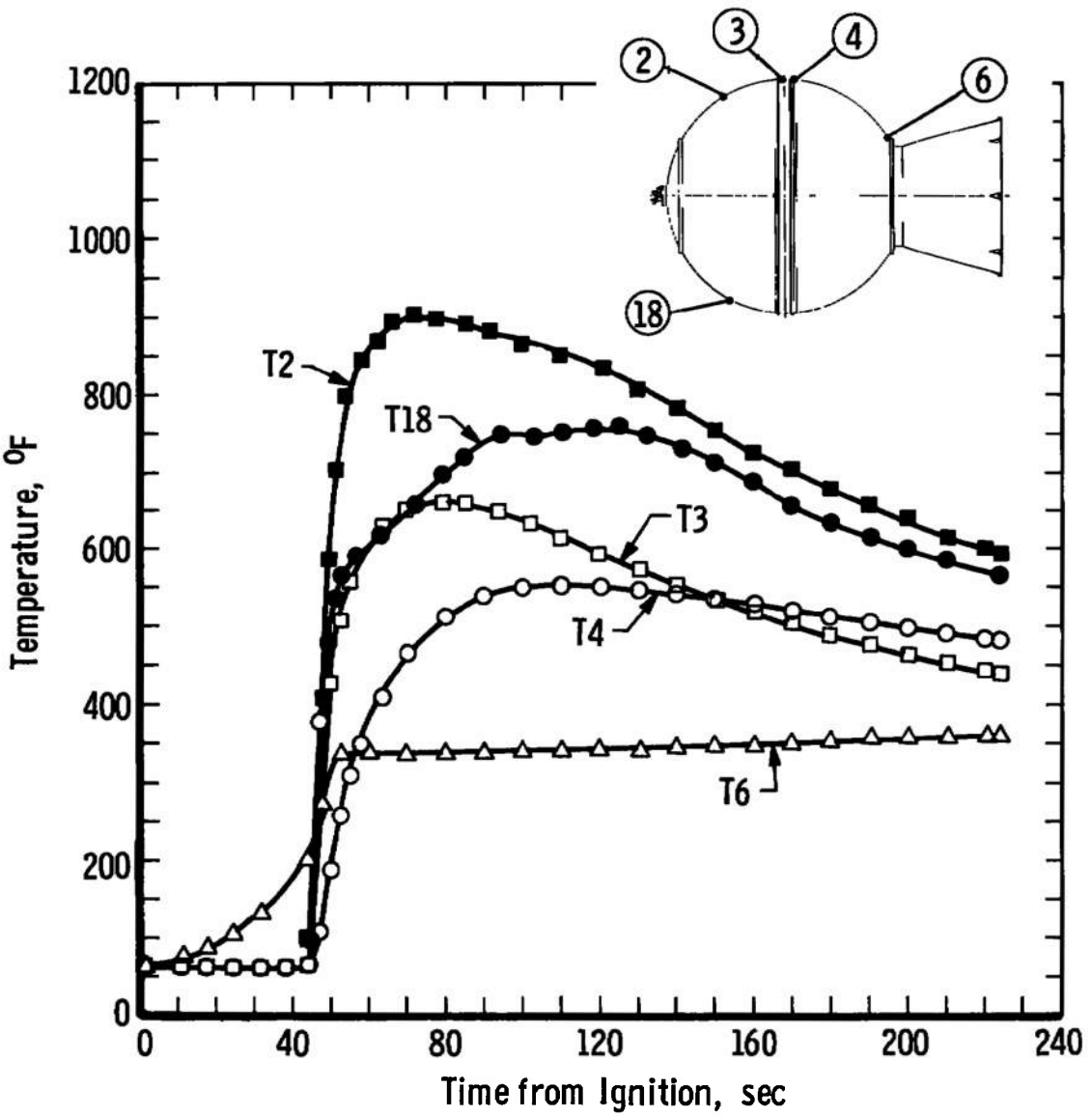

Fig. 17 Time Variation of Typical Motor Case (Midsection and Nozzle Adapter Flange) Temperatures

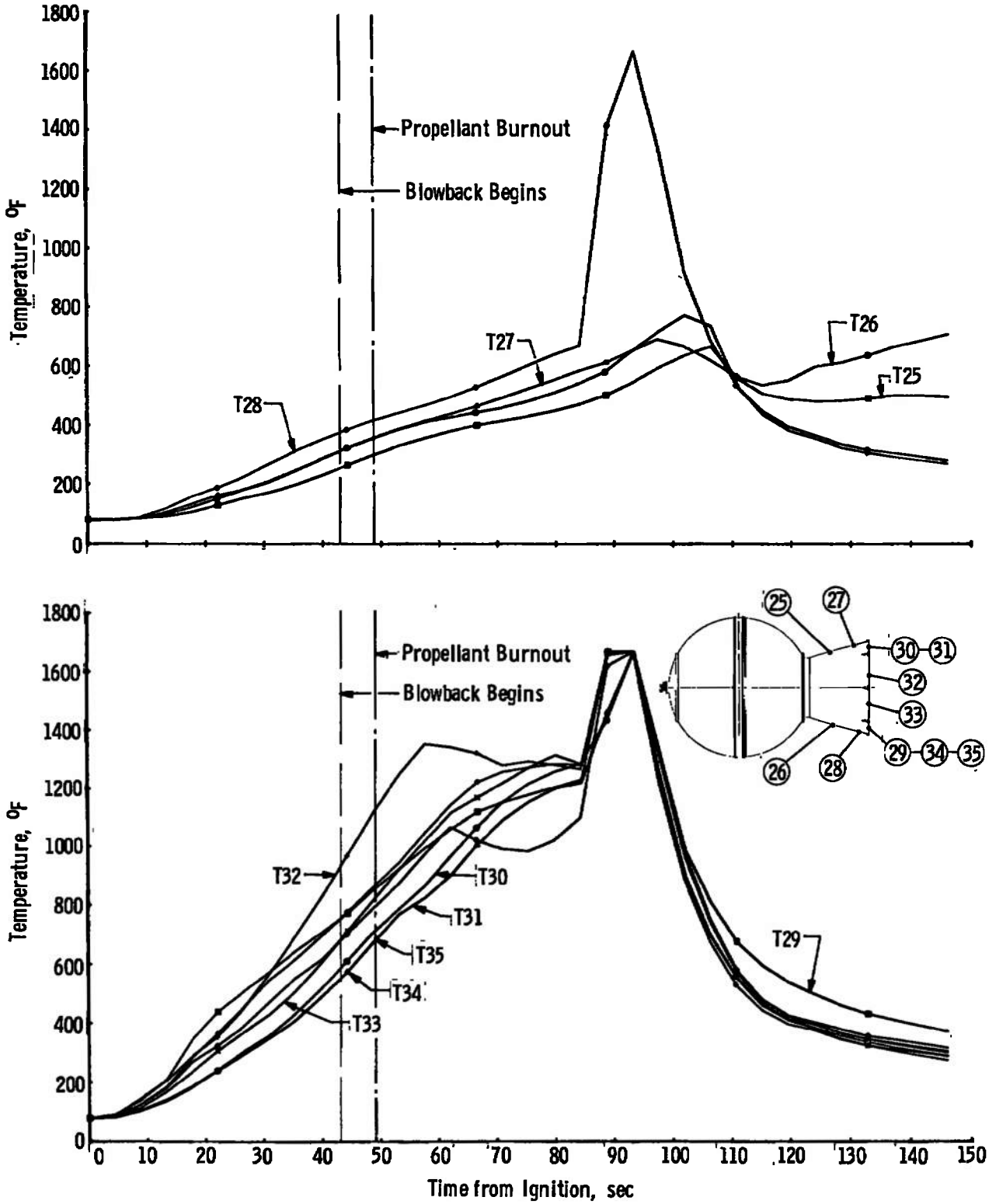

Fig. 18 Time Variation of Typical Nozzle Temperatures

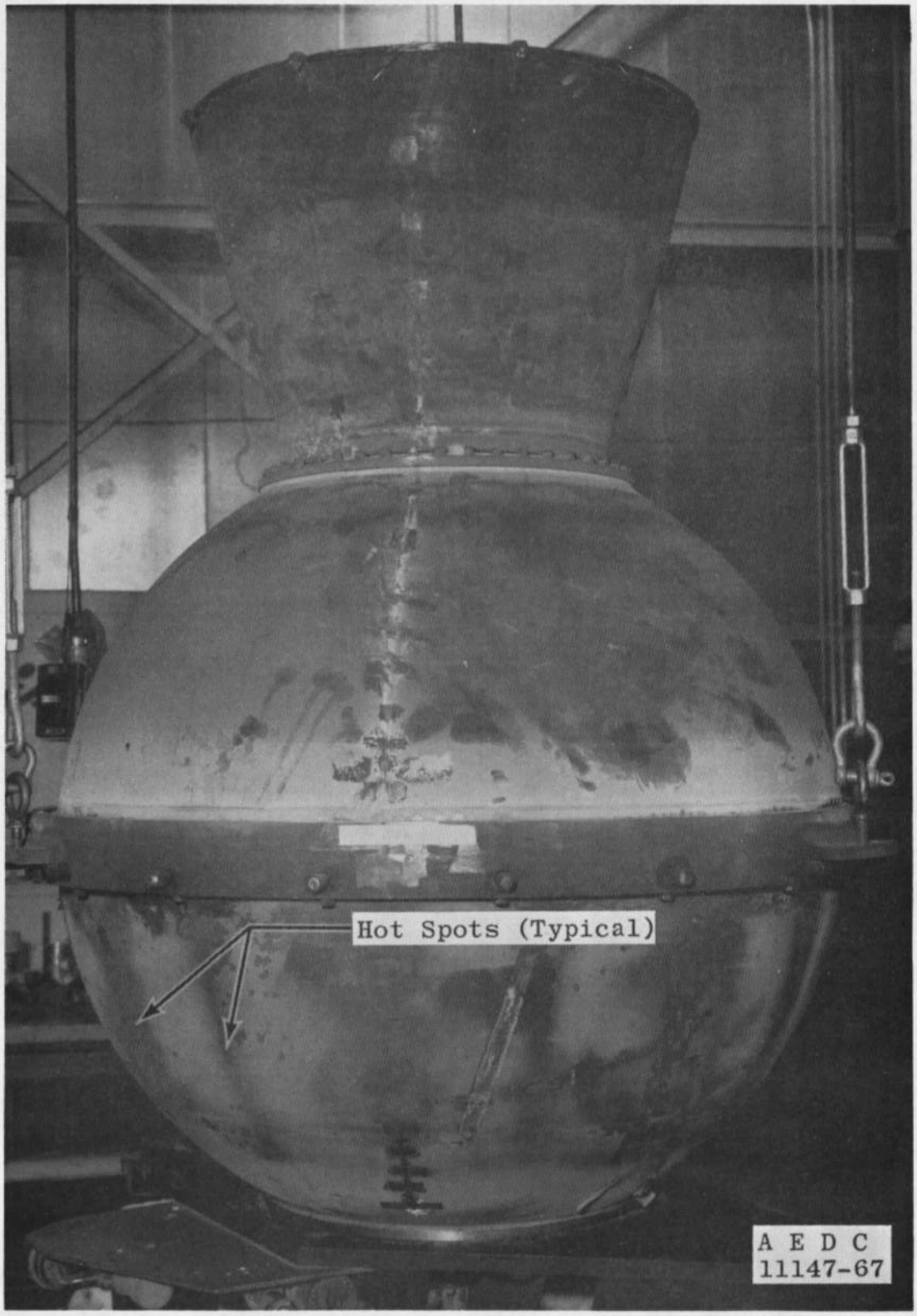

Fig. 19 Post-Fire Photograph of Motor S/N T00001 Showing Hot-Spots on Forward Hemisphere

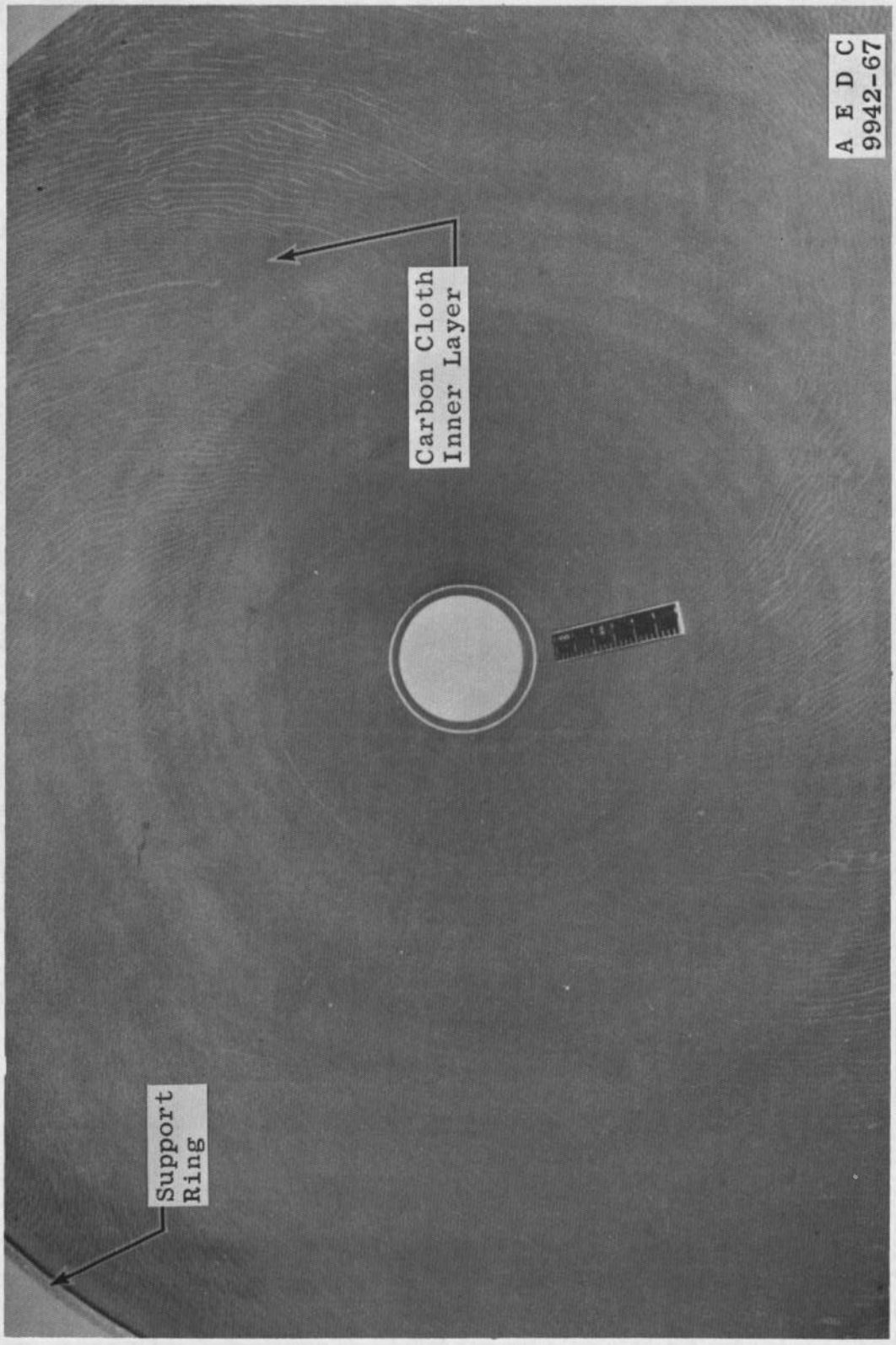

a. Typical Pre-Fire

Fig. 20 Nozzle Exit Cone Interior Condition

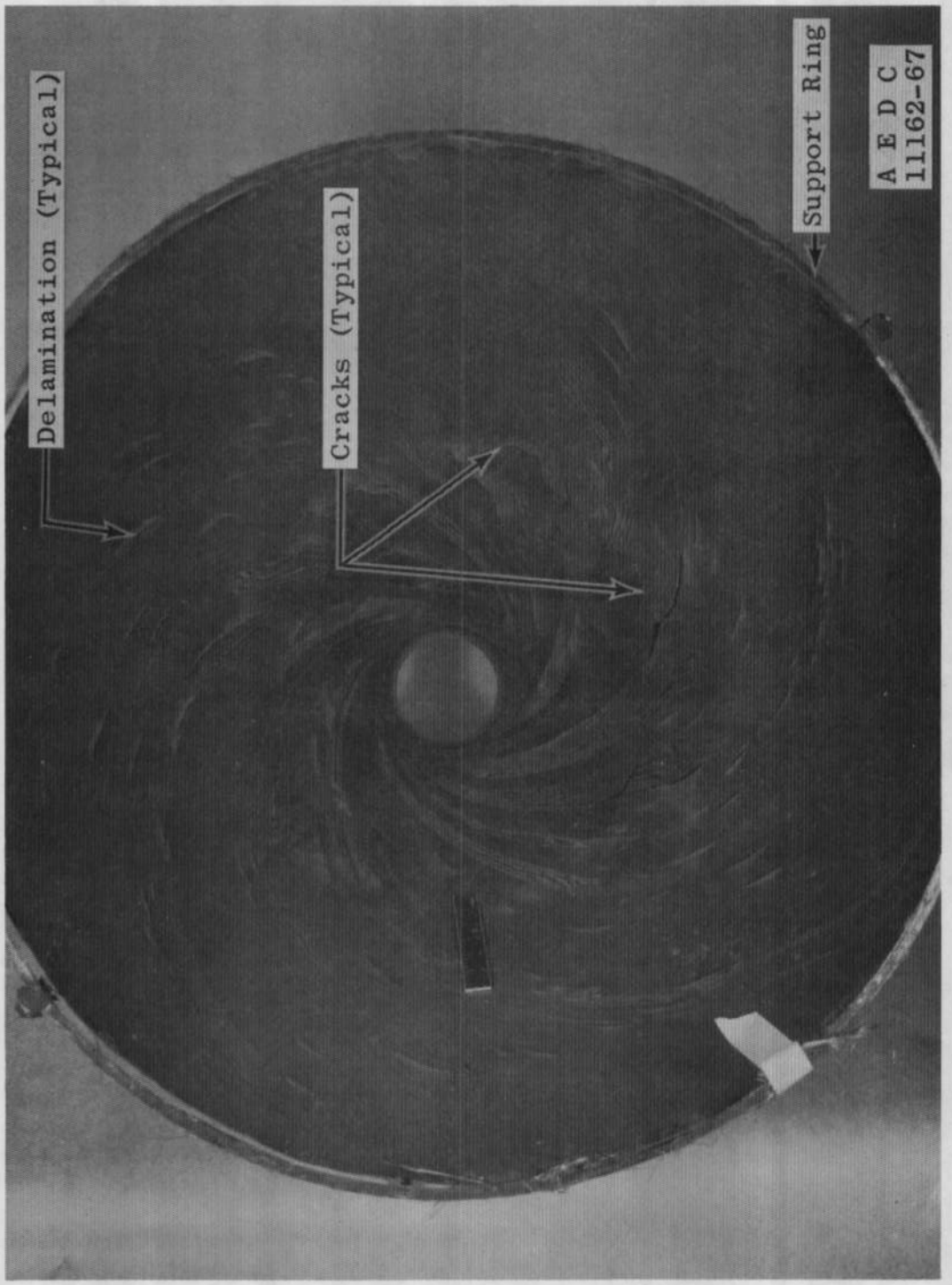

b. Post-Fire Motor S/N T00001
Fig. 20 Continued

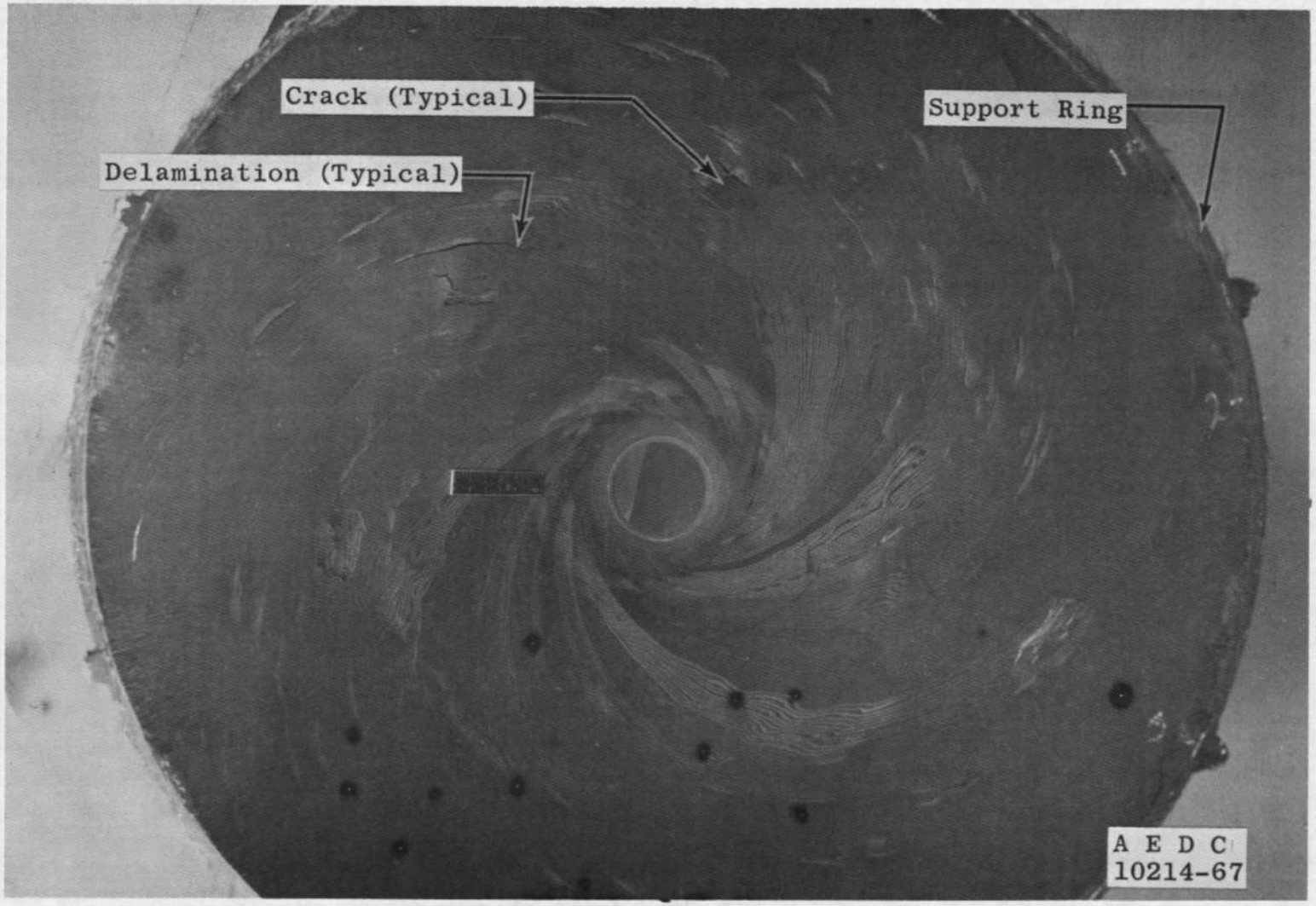

c. Post-Fire Motor S/N T00002

Fig. 20 Continued

d. Post-Fire Motor S/N T00003

Fig. 20 Continued

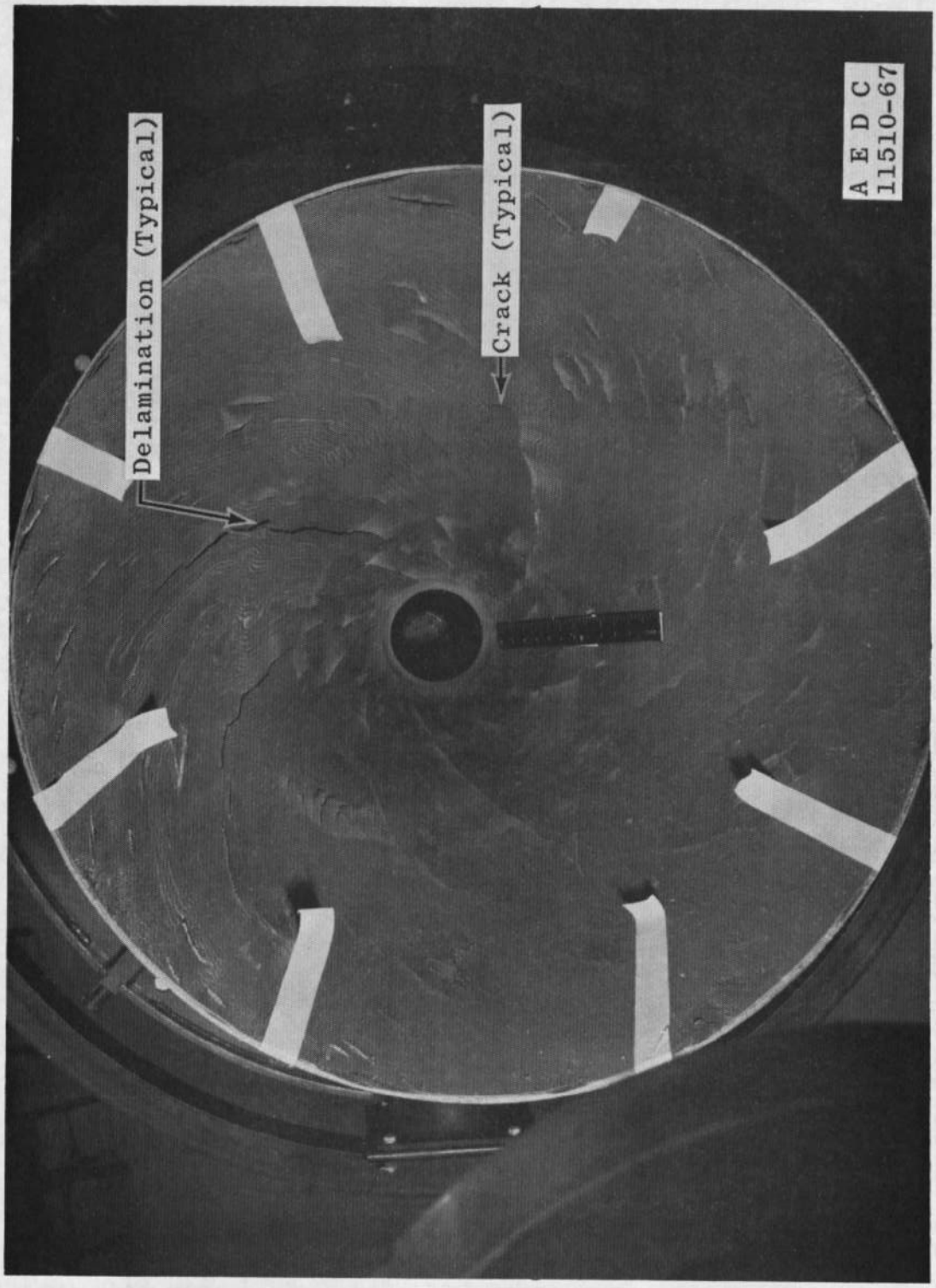

e. Post-Fire Motor S/N T00006

Fig. 20 Concluded

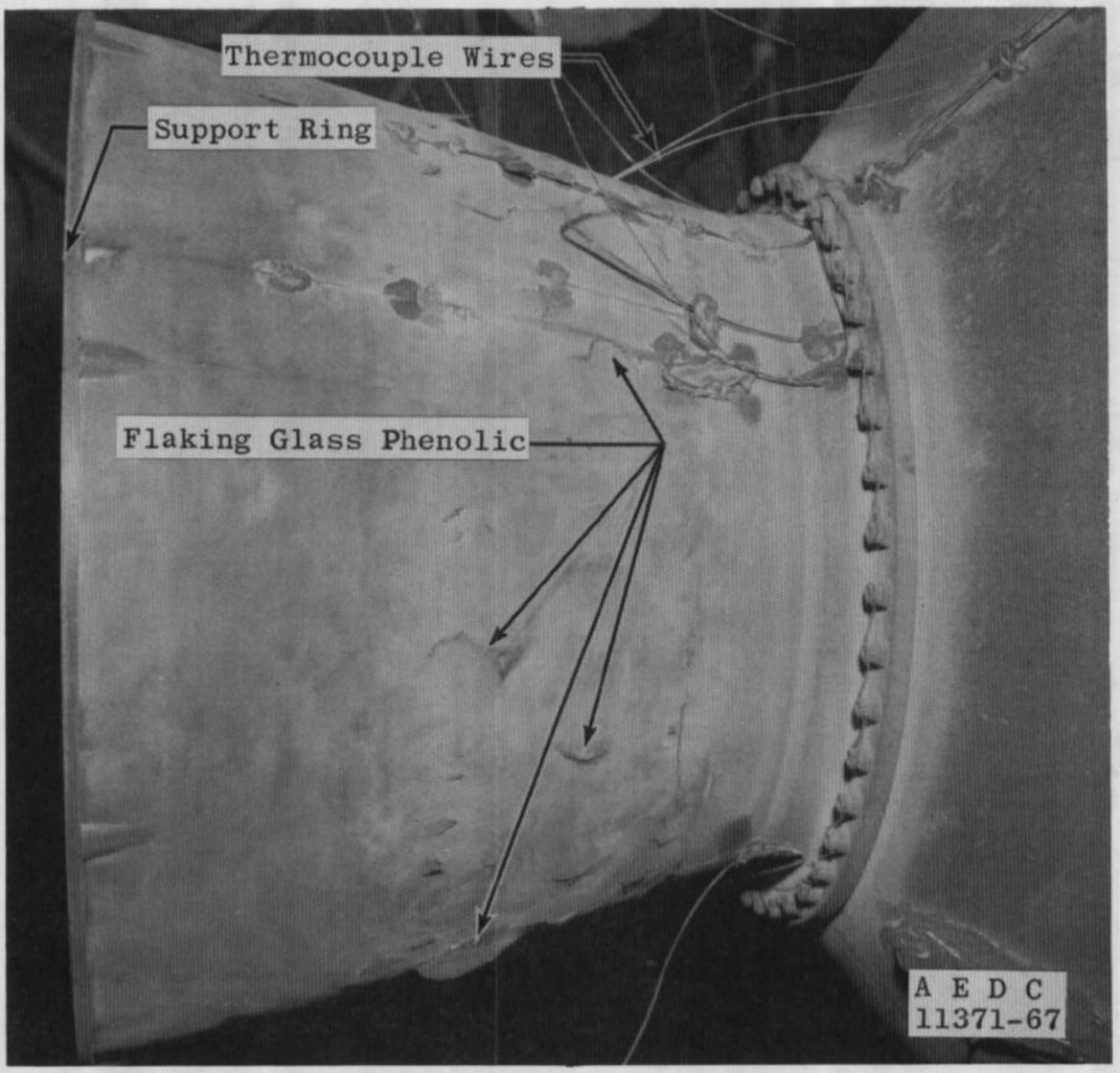

Fig. 21 Typical Nozzle Exit Cone Exterior Condition

TABLE I
INSTRUMENTATION DESCRIPTION

Parameter	Estimated Measurement Uncertainty (2 Sigma)				Range of Measurement	Type Measuring Device	Recording Device	Method of System Calibration
	Steady State at Operate Level, Percent of Reading	Integral, Percent of Reading	Over the Range of Measurement				Type	
			Percent of Reading	Units of Measurement				
Axial Force, lb_f	±0.33	---	---	---	0 to 10k lb_f	Bonded Strain-Gage Force Transducer (2 used)	Voltage-to-Frequency Converter Onto Magnetic Tape	Deadweight
Total Impulse, lb_f-sec	---	±0.32	---	---				
Motor Chamber Pressure, psia	±0.29	---	---	---	0 to 600 psia	Bonded Strain-Gage Pressure Transducer (2 used)		Resistance Shunt
Chamber Pressure Integral, psia-sec	---	±0.24	---	---				
Low-Range Chamber Pressure, psia	---	---	±0.50	---	15 to 50 psia	(1 used)		
	---	---	±0.50	---	5 to 15 psia	(1 used)		
	---	---	±0.50	---	1 to 5 psia	(1 used)		
Test Cell Pressure, psia	±1.47	---	---	---	0 to 0.1 psia	Unbonded Strain-Gage Pressure Transducer (3 used)		
Test Cell Pressure Integral, psia-sec	---	±1.46	---	---				
Event Time, msec	---	---	---	±5 msec	---	Synchronous Timing-Line Generator	Photographically Recording Galvanometer Oscillograph	Compared to Frequency Standard
Temperature, °F	---	---	---	±11°F	0 to 2300°F	Chromel-Alumel Temperature Transducers	*	Millivolt Source and NBS Temperature Tables
Weight, lb_m	---	---	---	±0.03 lb_m	0 to 3000 lb_m	Beam Balance Scales	Visual Readout	Periodic Deadweight Calibration

*Sequential Sampling Millivolt-to-Digital Converter and Magnetic Tape Storage Data Acquisition System

TABLE II
SUMMARY OF TE-M-364-3 MOTOR PHYSICAL DIMENSIONS

Test Number	3	4	5	6
Motor Serial Number	T00002	T00003	T00001	T00006
Test Date	8/9/67	8/15/67	8/23/67	8/30/67
Average Motor Spin Rate during Firing, rpm	110.87	0	110.37	111.24
AEDC Pre-Fire Motor Weight, lb_m	1574.12	1575.40	1575.56	1575.02
AEDC Post-Fire Motor Weight, lb_m	122.54	121.93	123.18	122.64
AEDC Expended Mass, lb_m	1451.58	1453.47	1452.38	1452.38
Manufacturer's Stated Propellant Weight, lb_m	1438.72	1440.60	1439.40	1439.91
Nozzle Throat Area, $in.^2$				
Pre-Fire	8.486	8.501	8.496	8.491
Post-Fire	9.239	9.445	9.234	9.253
Percent Change from Pre-Fire Measurement	+8.88	+11.1	+8.69	+8.97
Nozzle Exit Area, $in.^2$				
Pre-Fire	457.158	455.303	457.151	454.592
Post-Fire	457.840	456.988	459.580	453.333
Percent Change from Pre-Fire Measurement	+0.15	+0.37	+0.53	-0.28
Nozzle Area Ratio				
Pre-Fire	53.87	53.32	53.81	53.54
Post-Fire	49.55	48.38	49.77	48.99
Average	51.71	50.85	51.79	51.265

TABLE III
SUMMARY OF TE-M-364-3 MOTOR PERFORMANCE

Test Number RC1707	3	4	5	6
Motor Serial Number	T00002	T00003	T00001	T00006
Test Date	8/9/67	8/15/67	8/23/67	8/30/67
Pre-Fire Grain Temperature, °F	95 ± 5	75 ± 5	55 ± 5	50 ± 5
Average Motor Spin Rate during Firing, rpm	110.87	0	110.37	111.24
Simulated Altitude at Ignition, ft	112,000	123,000	121,000	124,000
Ignition Lag Time (t_ℓ)[1], sec	14.815	15.411	15.825	15.948
Action Time (t_a)[1], sec	43.5	45.0	45.6	46.1
t_{is} Burn Time[1], sec	100.8	100.8	121.6	111.85
Average Simulated Altitude during t_a, ft	88,000	104,000	105,000	105,000
Peak Pyrogen Pressure during Ignition Event, psia	1222	1254	1179	1211
Measured Total Impulse (Based on t_a), lb_f-sec				
Average of Three Channels of Data	412,028	414,848		
Average of Four Channels of Data			413,998	413,756
Maximum Deviation from Average, percent	0.012	0.005	0.003	0.010
Chamber Pressure Integral (Based on t_a), psia-sec				
Average of Two Channels of Data	25,344	25,100	25,242[4]	25,259
Maximum Deviation from Average, percent	0.012	0.022	0.28	0.012
Cell Pressure Integral (Based on t_a), psia-sec				
Average of Three Channels of Data	12.326	6.1422	5.9376	6.0445[3]
Maximum Deviation from Average, percent	1.00	0.21	0:099	
Vacuum Total Impulse (Based on t_a), lb_f-sec	417,667	417,650	416,720	416,500
Vacuum Total Impulse (Based on t_{is})[2], lb_f-sec	419,426	419,531	418,861	418,133
Vacuum Specific Impulse (Based on t_a), lb_f-sec/lb_m				
Based on Manufacturer's Stated Propellant Weight	290.30	289.91	289.51	289.25
Based on Expended Mass (AEDC)	287.73	287.35	286.92	286.77
Vacuum Specific Impulse (Based on t_{is}), lb_f-sec/lb_m				
Based on Manufacturer's Stated Propellant Weight	291.53	291.22	291.00	290.39
Based on Expended Mass (AEDC)	288.94	288.64	288.40	287.90
Average Vacuum Thrust Coefficient, C_F				
Based on t_a and Average Pre- and Post-Fire Throat Areas	1.859	1.854	1.862[4]	1.858
Maximum Motor Case Temperatures, °F	776	668	903	840
Time from Ignition that Maximum Motor Case Temperature Occurred, sec	82	104	72	60

[1]See nomenclature for definitions

[2]See Section 4.2 for method of calculation

[3]Only one channel of cell pressure available

[4]Chamber pressure measured through pyrogen

APPENDIX III
CALIBRATION OF NONAXIAL THRUST VECTOR MEASURING SYSTEM TO DETERMINE SYSTEM ACCURACY

To determine the accuracy of nonaxial thrust vector measurement using the spin technique, a spin calibration of the test configuration was accomplished. A description of the calibration technique used for the test reported herein is presented in the following sections.

INSTALLATION

The spin fixture was mounted on the thrust cradle with the spin axis aligned with the axial thrust column centerline. Forward and aft nonaxial force measuring load cells (0 to 500 lb_f) were mounted in the plane of the spin fixture horizontal centerline as shown in Fig. 4c. A stiffness check was made on the spin fixture-thrust cradle configuration which consisted of moving the assembly laterally off the aligned position a known amount and measuring the force exerted by the assembly on the load cells.

The motor and mounting can assembly was installed on the spin fixture, and the motor centerline was concentrically aligned with the axis of the spin fixture.

The entire system (thrust cradle, spin fixture, and motor) was aligned so that horizontal (lateral) force, as indicated by either the forward or aft nonaxial force load cell, was minimum (mechanical null position).

CALIBRATION PROCEDURE

A stand static calibration to determine system response to static, lateral loads was accomplished. This consisted of applying known lateral forces to the mounting can with and without an axial load of 11,000 lb_f applied to the system. The lateral loads were applied in the horizontal plane normal to the motor thrust axis near the plane of the nozzle throat. A comparison of measured and applied static force is presented in Fig. III-1. The measured force was, in all cases, greater than the applied force because, as the system is forced away from its mechanical null position, a weight component of the system, greater than the flexure restoring force, was imposed in addition to, and in the same direction as, the applied force. The deviation of measured from

applied static force was smaller during the post-fire calibration because the total system mass was less, decreasing the measured weight component of the system.

After the stand static calibration, the motor was rotated at 110 rpm about its axial centerline and balanced to a degree where the total nonaxial force produced by system unbalance was 0.35 lb_f. A dynamic (spin) calibration was then performed. This calibration consisted of placing known weights at several angular locations on the mounting can surface to produce a known nonaxial force as a function of spin rate:

$$F = mr\omega^2$$

where:

F = applied nonaxial force, lb_f

m = applied mass, lb_m

r = radial distance to center of gravity of applied mass, ft

ω = rotational speed, radians/sec

Two weights (nominally 1 and 2 lb_m) were attached to the can at 0 deg (pre-fire) and at three different angular locations (0, 60, and 120 deg), post-fire. Both the pre- and post-fire dynamic calibrations were conducted with and without axial loads applied.

DATA ACQUISITION AND REDUCTION

Applied Nonaxial Force

The applied nonaxial force was determined from the relationship:

$$F = \left[\frac{x}{x_o}\right] mr_{(app)}\omega^2$$

where $mr_{(app)}$ is the applied unbalance (product of applied mass and its radial distance) and ω is the rotational speed. The ratio $\left(\frac{x}{x_o}\right)$ is the magnification factor of forced vibration and is a function of the ratio of spin frequency (ω) to stand natural frequency (ω_n) as:

$$\frac{x}{x_o} = \frac{1}{\sqrt{\left[1 - \left(\frac{\omega}{\omega_n}\right)^2\right]^2 + \left[2\zeta \frac{\omega}{\omega_n}\right]^2}}$$

(the damping factor, ζ, was assumed to be zero). The ratio $\left(\frac{x}{x_o}\right)$ changed from pre- to post-fire because of the change in system natural frequency as a result of the change in mass.

Measured Nonaxial Force

Nonaxial force data were recorded on magnetic tape during the calibration sequence. These data were then electronically filtered to remove all frequencies above the rotational frequency.

The nonaxial force magnitude and angular location were corrected for filter effects as outlined in Ref. 5.

The measured force (determined from stand static calibration results) consisted of the force due to the applied weight and the residual unbalance force in the system. The true measured nonaxial force resulted when the residual unbalance force was vectorially subtracted from the measured force.

RESULTS

Figure III-1 is a comparison of measured and applied static force for the calibration reported herein. The application of 11,000-lb_f axial load to the system had no effect on the slope of either the pre- or post-fire calibration curves. The ratios of measured to applied static force were 1.030 pre-fire and 1.008 post-fire.

Nominal unbalances of 11.5 and 30 in.-lb_m were applied at an angular location of 0 deg during the pre-fire spin calibration. The system was then rotated at 110 (11.5 and 30 in.-lb_m) and 150 (11.5 in.-lb_m unbalance, only) rpm.

The post-fire calibration consisted of applying nominal unbalances of 11.5, 30, and 50 in.-lb_m at angular locations of 0, 60, and 120 deg. The system was then rotated at 110 rpm.

A comparison of true measured and applied nonaxial force is presented in Fig. III-2. The true measured force presented is an average of 10 values. Typical envelopes of the data points used in the averages are presented and incorporated into the accuracy determination. The maximum deviation of true measured from applied nonaxial force of 0.60 lb_f was observed at an applied nonaxial force of 8.50 lb_f. The system accuracy, based on an estimated two-standard deviation for the test reported herein, was ±0.80 lb_f at the steady-state thrust level.

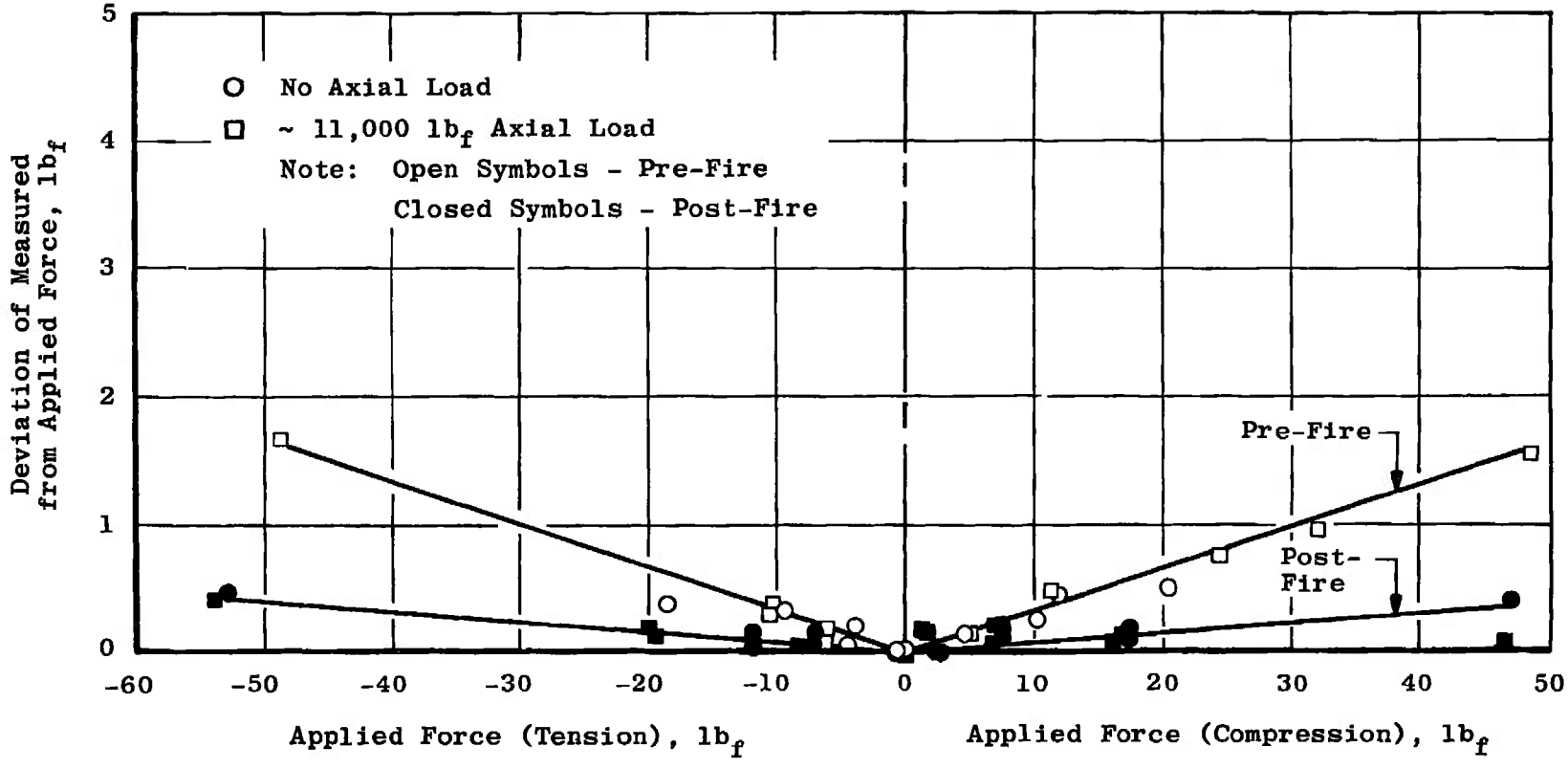

Fig. III-1 Comparison of Measured and Applied Static (Lateral) Force for Pre- and Post-Fire Motor S/N T00005

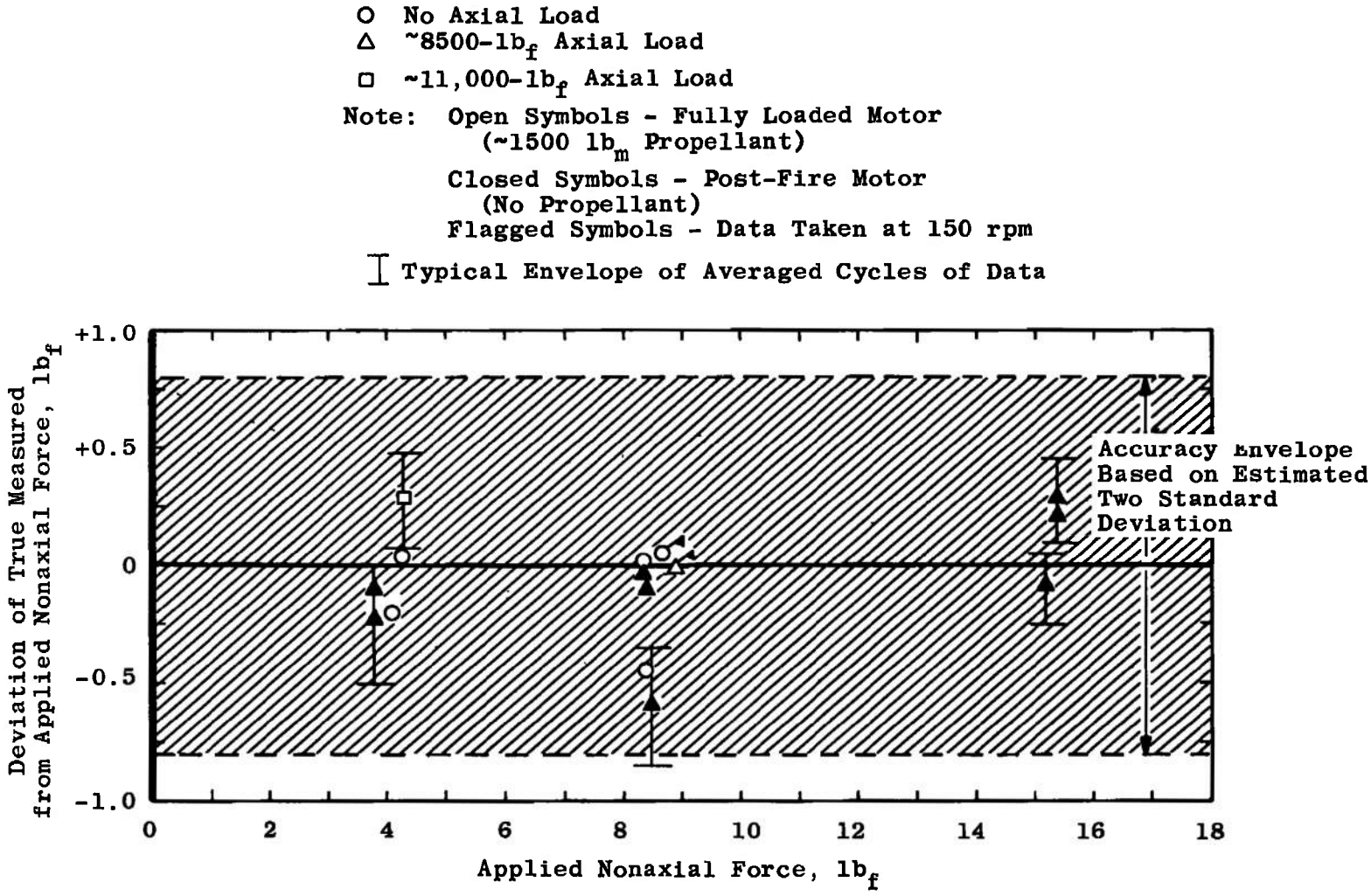

Fig. III-2 Comparison of True Measured and Applied Nonaxial Force Values for Spin Calibration to Determine System Accuracy

Security Classification

DOCUMENT CONTROL DATA - R & D

(Security classification of title, body of abstract and indexing annotation must be entered when the overall report is classified)

1 ORIGINATING ACTIVITY (Corporate author)	2a. REPORT SECURITY CLASSIFICATION
Arnold Engineering Development Center ARO, Inc., Operating Contractor Arnold Air Force Station, Tennessee	UNCLASSIFIED
	2b. GROUP N/A

3 REPORT TITLE

QUALIFICATION TESTS OF THIOKOL CHEMICAL CORPORATION TE-M-364-3 SOLID-PROPELLANT ROCKET MOTORS TESTED IN THE SPIN AND NO-SPIN MODE AT SIMULATED ALTITUDE CONDITIONS (PART II - FINAL PHASE)

4. DESCRIPTIVE NOTES (Type of report and inclusive dates)

August 9 to 30, 1967 - Final Report

This document has been approved for public release ~~its distribution is unlimited~~.

5. AUTHOR(S) (First name, middle initial, last name)

D. W. White and J. E. Harris, ARO, Inc.

6 REPORT DATE	7a. TOTAL NO. OF PAGES	7b. NO. OF REFS
January 1968	70	5

8a. CONTRACT OR GRANT NO.	9a. ORIGINATOR'S REPORT NUMBER(S)
AF 40(600)-1200 b. PROJECT NO 9033 c. System 921E d.	AEDC-TR-67-256
	9b. OTHER REPORT NO(S) (Any other numbers that may be assigned this report) N/A

10 DISTRIBUTION STATEMENT

Subject to special export controls; transmittal to foreign governments or foreign nationals requires approval of NASA, Goddard Space Flight Center, Greenbelt, Maryland.

11. SUPPLEMENTARY NOTES	12. SPONSORING MILITARY ACTIVITY
Available in DDC	NASA, Goddard Space Flight Center Greenbelt, Maryland

13 ABSTRACT

A qualification test program consisting of six Thiokol Chemical Corporation TE-M-364-3 solid-propellant rocket motors was conducted at near vacuum conditions to determine altitude ballistic performance, nonaxial thrust of the spinning motors, tailoff characteristics, temperature-time history during and after motor operation, and component structural integrity. The initial phase of the program consisted of firing one motor in the spin mode and one motor in the no-spin mode. The final phase consisted of firing three motors in the spin mode and one motor in the no-spin mode. The vacuum total impulse values of all motors were within the specification limits. Nonaxial thrust impulse values of the spinning motors and the maximum motor case temperatures for all motors exceeded the specification limit.

DD FORM 1 NOV 65 1473

Security Classification

Security Classification

14. KEY WORDS	LINK A		LINK B		LINK C	
	ROLE	WT	ROLE	WT	ROLE	WT
solid propellants						
rocket motors						
spin tests						
temperature						
performance						
structural integrity						

1. SPR motors -- Quality acceptance testing

2. " " -- Performance

3. " " -- Spinning.

16. 3.

Security Classification

ERRATA

AEDC-TR-67-256, January 1968
(UNCLASSIFIED REPORT)

QUALIFICATION TESTS OF THIOKOL CHEMICAL CORPORATION TE-M-364-3 SOLID-PROPELLANT ROCKET MOTORS TESTED IN THE SPIN AND NO-SPIN MODE AT SIMULATED ALTITUDE CONDITIONS (PART II - FINAL PHASE)

D. W. White and J. E. Harris, ARO, Inc.

Arnold Engineering Development Center
Air Force Systems Command
Arnold Air Force Station, Tennessee

The following figure replaces Fig. 18, p. 47:

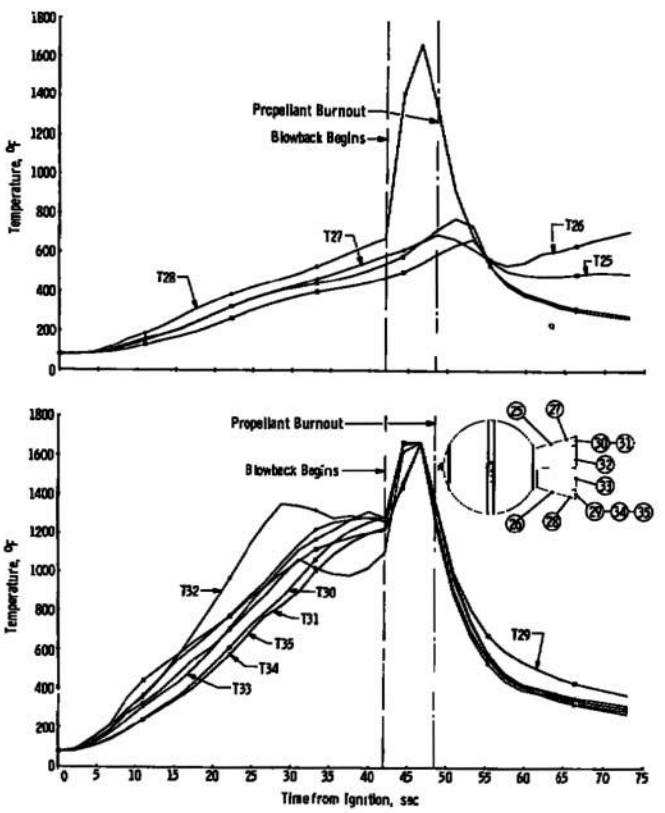

Fig. 18 Time Variation of Typical Nozzle Temperatures